Bifunctional homogeneous catalysts based on first row transition metals in asymmetric hydrogenation

Francine Agbossou-Niedercorn,[a,*] Christophe Michon[a,b,*]

Addresses:

Dr. Francine Agbossou-Niedercorn,[a,*] Dr. Christophe Michon[a,b,*]

a) Univ. Lille, CNRS, Centrale Lille, Univ. Artois, UMR 8181 - UCCS

- Unité de Catalyse et Chimie du Solide, F-59000 Lille, France.

b) Dr. Christophe Michon (new adress)

Université de Strasbourg, Université de Haute-Alsace,

Ecole Européenne de Chimie, Polymères et Matériaux, CNRS, LIMA, UMR 7042,

25 rue Becquerel, 67087 Strasbourg, France.

Email: francine.niedercorn@univ-lille.fr / cmichon@unistra.fr

Keywords:

Asymmetric hydrogenation, bifunctional catalyst, cobalt, iron, manganese, nickel

Abstract.

This article reviews over the past 10 years the development of bifunctional homogeneous catalysts based on first row transition metals for asymmetric hydrogenation of various CC, CO and CN double bonds. Following the impressive performances of ruthenium based bifunctional catalysts in asymmetric transfer hydrogenation and asymmetric hydrogenation and, because of economic, environmental and societal reasons, bifunctional catalysts based on abundant metals and mainly on the first row transition metals have gradually been developed over the last decade. Hence, several bifunctional catalysts based on iron, manganese, cobalt and nickel have been reported and promising activities and enantioselectivities have already been achieved. This review highlights and discusses the reactivity and performances of these new bifunctional catalysts as well as the implied reaction mechanisms.

Contents:

Abreviations:

AH: asymmetric hydrogenation
ATH: asymmetric transfer hydrogenation
BINAP: 1,1′-Binaphthalene-2,2′-diyl)bis(diphenylphosphine)
cat: catalyst
COD: cyclooctadiene
conv: conversion
de: diastereomeric excess
DKR: dynamic kinetic resolution
DPEN: diphenylethylenediamine
dr: diastereomeric ratio
ee: enantiomeric excess
HFIP: hexafluoroisopropanol
NMR: Nuclear Magnetic Resonance
THF: tetrahydrofurane
TOF: turnover frequency
TON: turnover number
TRIP: 3,3'-bis(2,4,6-triisopropylphenyl)-1,1'-binaphthyl-2,2'-diyl hydrogenphosphate

1. Introduction

Asymmetric hydrogenation (AH) is a fundamental chemical reaction which provides high degree of stereocontrol for the preparation of optically pure fine chemicals comprising pharmaceuticals, agrochemicals, flavours and fragrances. Many effective asymmetric hydrogenations of functionalized olefins and ketones were achieved in the presence of chiral homogeneous metal-based catalysts and several led to industrial productions of single enantiomers of advanced intermediates [1-13]. However, most of these catalytic synthetic methodologies were based on rhodium and relied on the coordination of a substrate's functional group on the reactive metal centre in order to facilitate and direct the hydride transfer into the unsaturated bond to be reduced [14]. Another drawback of the well developed rhodium enantioselective hydrogenation catalysts is their general inertness towards ketones [15].

In 1995, Noyori et al. reported a new catalyst based on a combination of ruthenium, BINAP, chiral diamine and KOH which was able to hydrogenate simple aromatic ketones with high stereoselectivity [16]. The same year, Noyori et al. made an important breakthrough by introducing a conceptually new chiral ruthenium catalyst containing *N*-sulfonylated 1,2-diamines or amino-alcohols as chiral ligands for highly efficient asymmetric transfer hydrogenation (ATH) of ketones [17]. Such ruthenium catalyst proceeded according to a bifunctional mechanism [18] through a six-membered pericyclic transition state entailing the metallic centre and a NH functionality of the diamino (or amino alcohol) ligand as observed for both AH [15,19] and ATH [20-21] of ketones. In particular, the reversible mechanism of these ruthenium bifunctional catalysts was confirmed by investigations on the half-sandwich catalyst structures and a better understanding of the mechanism of the hydrogen atom transfer [22] between alcohol reagent and ketone substrate through kinetic studies and isotope labelling [23-25] as well as computational analysis [26-28]. Hence, these ruthenium catalysts were shown to rely on the N-H ligand functionality which interacted with the metal centre in a cooperative manner along the hydrogenation reaction. In other words, such ruthenium catalysts offered a combination of Lewis acid and Lewis base working in concert with high efficiency [5,29-30]. The Noyori half-sandwich bifunctional catalysts are very effective for ATH and offer a great potential for high stereocontrolled syntheses using either 2-propanol, either an azeotropic mixture of formic acid and triethylamine as hydrogen source. It is worth to note such two costless, non-toxic and environmentally safe hydrogen sources do not require the use of specific equipments. In the case of 2-propanol, a drawback may be the thermodynamic reversibility of the transfer hydrogenation reaction leading to a limited conversion and therefore a decrease of

the enantiomeric purity of the targeted chiral alcohol. The use of formic acid and triethylamine can overcome the drawback of reversibility as the formed CO_2 can be removed during catalysis to lead to full conversion.

Since the first reports of Noyori et al., the promising application of bifunctional molecular metal catalysts in asymmetric hydrogenation and asymmetric transfer hydrogenation has inspired numerous academic researches focusing on the development of new catalysts based on late-transition metals and further applications in C-H, C-C, C-N, and C-O bond formation [31-38]. Due to their high potential and because of the continuous demand of new catalysts,[39] bifunctional catalysts applied in ATH and AH have remained of high interest over the last decade. Interestingly, this long-term interest for innovative hydrogenation catalytic systems has resulted in the discovery of metal catalysts exhibiting new functionalities. For example, bifunctional catalysts were sought to either activate the hydrogen source in a bifunctional manner [40] or to interact in a specific way through secondary interactions with the substrate for activation and/or structural benefits (cooperative catalysis) [41]. Furthermore, recent theoretical studies on hydrogenation catalysts have highlighted the significant contribution of weak non-covalent attractive interactions between the substrate and catalyst's chiral ligand to the enantioselective process [42-44]. Beside catalysts based on late-transition metals, attention has gradually turned on catalysts based on abundant and non-precious metals, i.e. first row transition metals, due to economic, environmental and societal reasons [45-49]. This trend has included the development of homogeneous bifunctional (cooperative) catalysts for AH and ATH [50-54] and this review will focus on the developments of such catalysts over the last ten years, i.e. along the 2010 - mid 2020 period. Manganese, iron, cobalt and nickel homogeneous bifunctional catalysts will only be considered focusing on the development of new catalytic systems and the deep understanding of the implied reaction mechanisms.

For clarity's sake, the readers will find below previous definitions of bifunctional catalysts:

1) According to T. Ikariya [55]: *"...bifunctional catalysts have two functionalities cooperating in substrate activation and transformation..."*

2) According to D. B. Grotjahn [56]: *"...organometallic catalysts resulting from including ligands capable of proton transfer or hydrogen bonding..."*

3) According to S. J. Miller [57]: *"Bifunctional catalysts usually possess a nucleophilic moiety appended to Lewis basic or Brønsted acidic moieties capable of hydrogen bonding or charge stabilization. Coupling of these functionalities typically results in cooperative activation of substrates and stabilization of transition states leading to heightened reactivity and higher levels of enantiocontrol in various transformations."*

2. First reports.

In parallel to the rise of ruthenium systems, bifunctional catalysts based on abundant metals have gradually been developed for asymmetric hydrogenation. To the best of our knowledge, the early examples appeared before 2010 and relied on cobalt and iron complexes as depicted below.

In 1997, Lemaire et al. reported a pioneering study on the application of cobalt(II) pre-catalyst (**1**) based on dimethylated diphenylethylene diamine (DPEN) ligand to the ATH of acetophenone (Scheme 1) [58]. Though modest, the conversions were increased with the base loading (8-30%) but the enantioselectivities (7-58% ee) decreased in parallel. Although activities were low and enantioselectivities average, these results were nonetheless encouraging at that time.
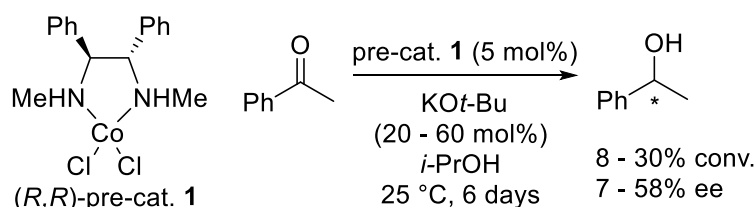
Scheme 1. ATH of acetophenone catalysed by chiral cobalt(II) pre-catalyst **1** by Lemaire et al.

A few years later, Gao et al. reported the ATH of various ketones through the use of in-situ prepared catalysts by combining PNHNHP ligand (**L1**) with the iron hydride cluster $[Et_3NH][HFe_3(CO)_{11}]$. The corresponding alcohols were obtained with promising conversions (up to 98%) and enantioselectivities (up to 98% ee) (Scheme 2) [59-60].
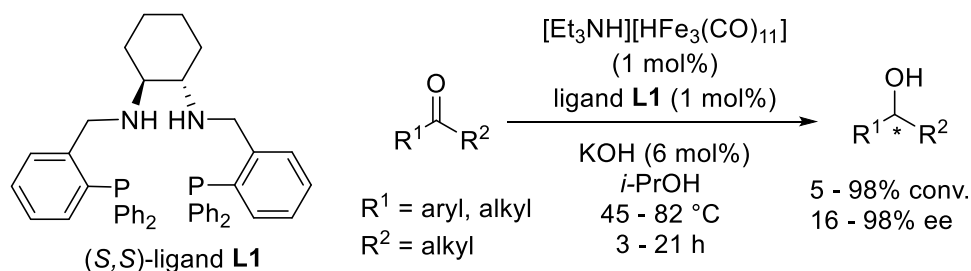
Scheme 2. ATH of ketones catalysed by a combination of chiral PNHNHP ligand **L1** and iron hydride cluster $[Et_3NH][HFe_3(CO)_{11}]$ by Gao et al.

In 2008, Morris et al. isolated well-defined chiral iron(II) complexes (**2**) bearing a PNNP tetradentate ligand as well as nitrile and carbonyl apical ligands and applied these species to the

ATH of a series of ketones (Scheme 3). While catalysts activities (26–995 h⁻¹ TOF) and yields (48-93%) were promising, enantioselectivities varied from low to high (12-96% ee) depending on the substrate [61-62].
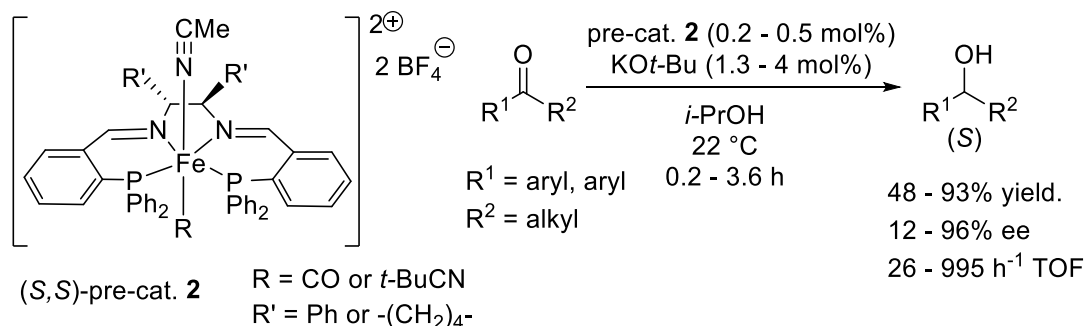
Scheme 3. ATH of ketones catalysed by chiral PNNP iron(II) pre-catalyst **2** by Morris et al.

Morris et al. subsequently prepared another well-defined chiral iron(II) complex (**3**) based on a new PNNP diiminodiphosphine ligand (Scheme 4). This catalyst was highly active in the ATH of a broad range of ketones, alcohols being obtained in high conversions (up to 99%) and low to good enantioselectivities (35-99% ee) depending on the substrate structure and steric hindrance. Afterwards, several experimental and theoretical studies highlighted the bifunctional behavior of these original iron catalysts and supported a reaction mechanism which will be adressed below [63-64].
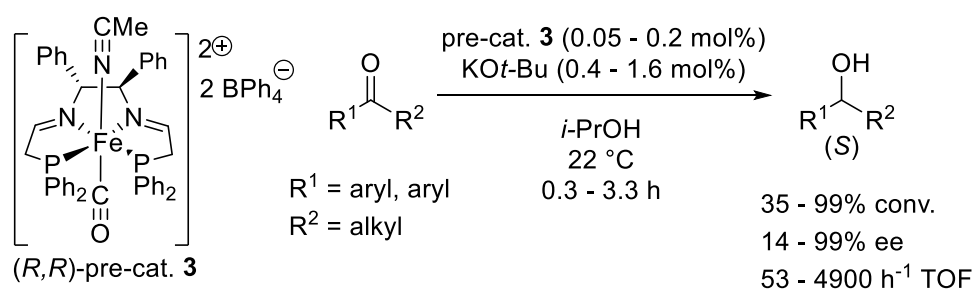

Scheme 4. ATH of ketones using chiral iron(II) pre-catalyst **3** based on a PNNP diiminodiphosphine ligand by Morris et al.

3. Asymmetric transfer hydrogenation.

3.1. Iron based catalysts.

3.1.1. Chiral Knölker-type complexes.

Inspired by the work of Knölker et al. who had reported a cyclopentadienone-iron complex active for the catalysed racemic transfer hydrogenations of CO and CN insaturations [65], Wills et al. reported the preparation of a range of diastereopure Knölker-type complexes (**4**) and (**5**), and their application to the ATH of acetophenone (Scheme 5) [66]. By requiring 48 or 96 hours of reaction, the catalyst activities were moderate and resulted in low to high conversions (10 to 91%) and modest enantioselectivities (5 to 25% ee). The enantioselectivity of the ATH was notably influenced by the catalyst single remote chiral centre and the complex planar chirality. Pre-catalysts (**4**) comprising methyl and $Fe(CO)_3$ on the same face of the cyclopentadienone ligand were the most selective. No racemization of catalysts was observed along the reactions.
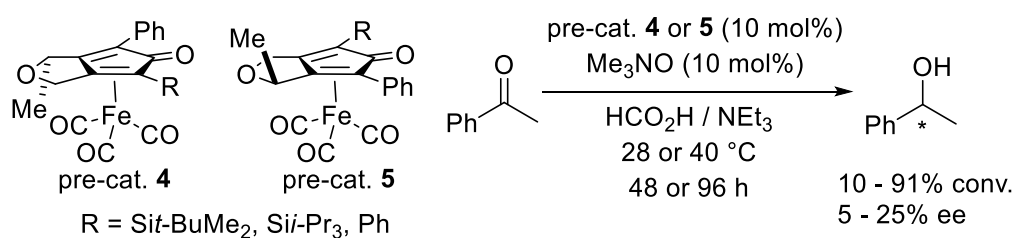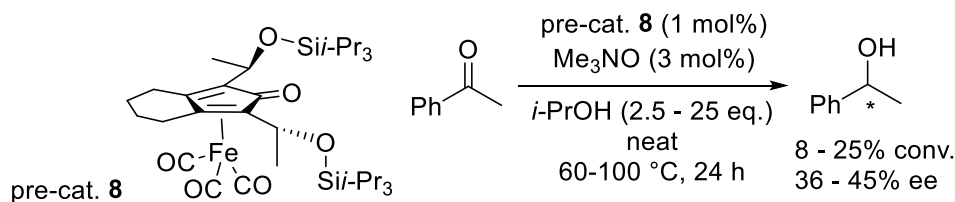

Scheme 5. ATH of acetophenone catalysed by diastereopure Knölker-type complexes **4** or **5** by Wills et al.

Afterwards, Wills et al. reported a series of enantiomerically-pure iron tricarbonyl cyclopentadienone complexes (**6**) and (**7**) (Scheme 6) [67]. Though all were active in the ATH of acetophenone (13-89% conv.), the enantiomeric excesses were low (2-35% ee). Catalysts bearing the bulkier silicon groups were the most selective. Furthermore, the derivatization of the catalysts by decarbonylation and coordination of a chiral Monophos phosphoramidite ligand resulted in poorly active species. Among the other prepared complexes, it was noticed a symmetrical substitution pattern around the ligand C=O bond by bulky anisole-type groups had a positive impact on the asymmetric induction (Scheme 6). Though the complexes (**7**) proved to be effective pre-catalysts for the reduction of acetophenone, the resulting 1-phenylethanol was formed in low ees.
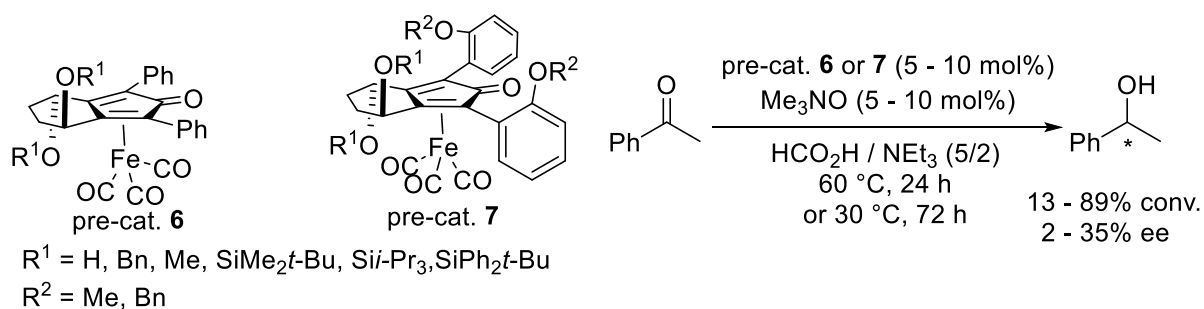
Scheme 6. ATH of acetophenone catalysed by enantiopure Knölker-type complexes **6** or **7** by Wills et al.

Recently, De Wildeman et al. prepared chiral Knölker-type complex (**8**) by functionalizing the cyclopentadienone ligand with chiral substituents on the 2- and 5-positions near the CO moiety (Scheme 7) [68]. The ATH of acetophenone was studied using controled amounts of isopropanol. Though the conversions were modest (8-25%), the enantioselectivities were among the highest obtained with a chiral Knölker catalyst (36-45% ee).

Scheme 7. ATH of acetophenone catalysed by enantiopure Knölker-type complex **8** by De Wildeman et al.

3.1.2. Iron catalysts based on chelate and macrocyclic ligands.

In 2010, Beller et al. reported the first iron-catalysed ATH of a range of *N*-(diphenylphosphinyl)ketimines (Scheme 8) [69]. The reaction operated in mild reaction conditions at rather low catalyst loadings by mixing iron carbonyl hydride cluster [Et$_3$NH][HFe$_3$(CO)$_{11}$] precursor with the selected diimine diphosphine PNNP tetradentate ligand (**L2**). At the exception of aliphatic imines, high yields and enantioselectivities were obtained.
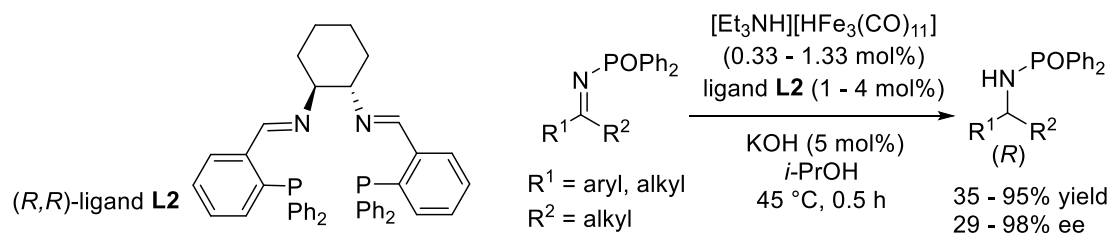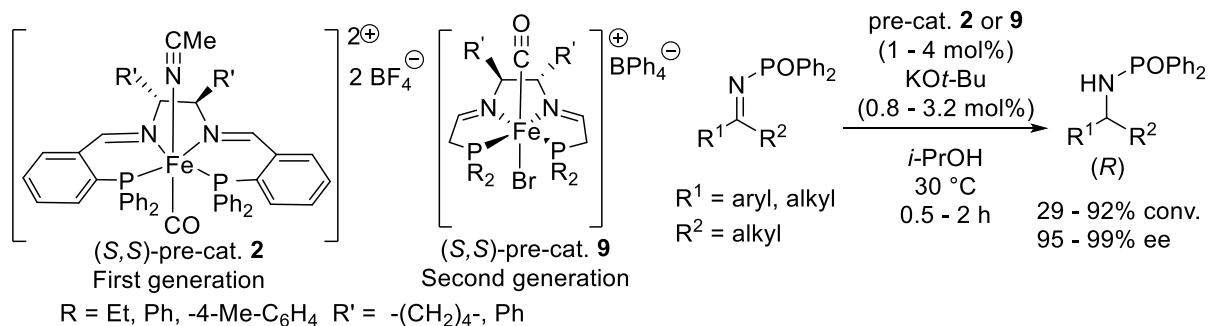
Scheme 8. ATH of *N*-(diphenylphosphinyl)ketimines catalysed by a combination of a chiral PNNP ligand **L2** and iron hydride cluster [Et$_3$NH][HFe$_3$(CO)$_{11}$] by Beller et al.

Starting from 2010, Morris et al. studied a series of *trans* iron(II) complexes (**9**) bearing tetradentate PNNP diiminodiphosphine ligands which featured different alkyl (Cy, *i*-Pr, Et) or aryl substituents at the phosphorus atoms (Scheme 9) [70-72]. Ligands bearing ethyl or aryl substituents resulted in active catalysts for ATH of acetophenone and PNNP phosphines with cyclohexyl or *iso*-propyl substituents led to inactive catalysts. However, 3,5-dimethyl-benzene substituents at the phosphorus atoms resulted in the most selective catalyst (82% ee) and the highest activity was reached using tolyl groups (4900 h^{-1} TOF). On the whole, these results underlined a fine balance between steric and electronic properties of the ligand was necessary to reach high activities and selectivities with this second generation of iron PNNP catalysts. The nature of the chiral diamine backbone had also a significant influence on the stereoselective outcome of the reductions, DPEN being the most suitable. Finally, the authors did not notice any significant difference of activity and selectivity between mono- and dicationic catalytic species, i.e. between iron complexes bearing bromide or acetonitrile ligands.
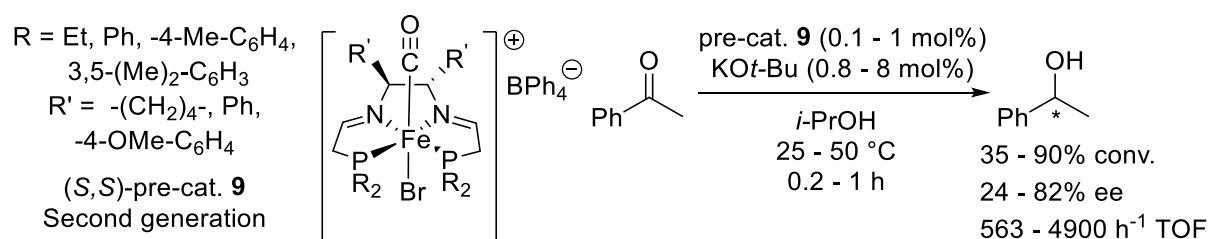
Scheme 9. ATH of ketones catalysed by iron(II) complexes **9** based on chiral PNNP ligands by Morris et al.

Afterwards, Morris et al. applied these *trans* iron complexes (**9**) to the ATH of a series of *N*-(diphenylphosphinyl)ketimines (Scheme 10) [73].

Scheme 10. ATH of *N*-(diphenylphosphinyl)ketimines catalysed by iron complexes **2** or **9** based on chiral PNNP ligands by Morris et al

The most active and enantioselective pre-catalyst was based on an alkyl skeleton comprising a DPEN chiral backbone and phenyl substituents at the phosphorus atoms. The reaction operated in mild reaction conditions at rather low catalyst loadings and led to average to good yields and high enantioselectivities.

By combining experimental and kinetic studies as well as theoretical calculations, Morris et al. investigated the reaction mechanism of the ketone ATH in the presence of second generation iron catalysts (Scheme 11) [74-76].
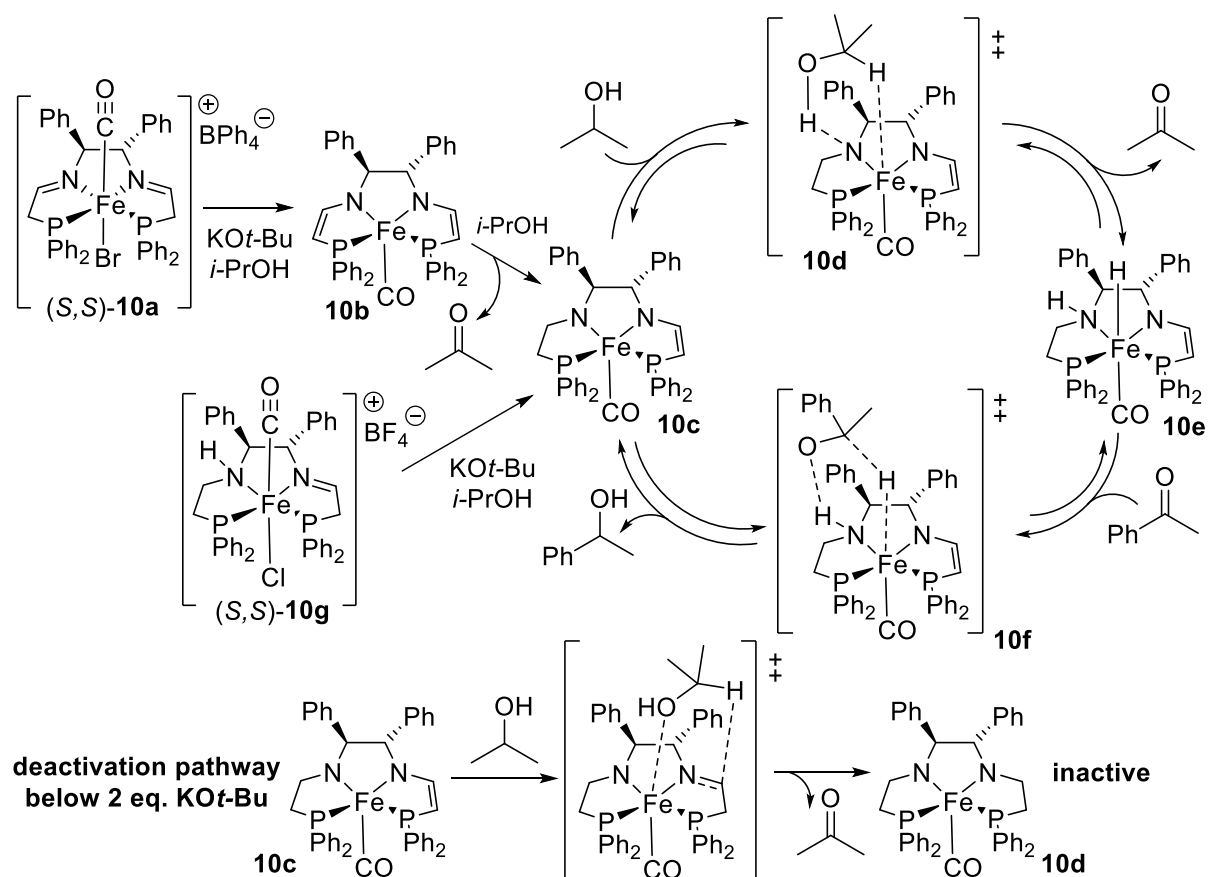
Scheme 11. Mechanism of the ATH of ketones catalysed by iron complex **10a** based on a chiral PNNP ligand by Morris et al.

At first, they noticed a modification of the pre-catalyst ligand before the reaction start. Indeed, the excess of strong base (KOt-Bu, NaOt-Bu, or KOH) which was required to activate the pre-catalyst (**10a**) reacted with the acidic hydrogens of the methylene groups next to the phosphines and led to a bis-enamide complex (**10b**) [77]. By providing a proton and a hydride, 2-propanol subsequently enabled the hydrogenation of one enamido moiety and led to the active (amido)(enamido)iron complex (**10c**) with the ligand thus hydrogenated on one side. A further reduction of the second enamido was possible while using less than 2 equivalents of base and resulted in an inactive bis(amido)species (**10d**). Hence, the catalytic ATH proceeded from the mono-enamide species in a similar mechanism than the ruthenium bifunctional catalysts: the iron centre and amido moiety receiving respectively a hydride and a proton from the 2-propanol solvent and the hydride transfer being the turn-over limiting step (Scheme 11, **10d**). The resulting (*S,S*)-(amine)(eneamido)iron hydride species (**10e**) subsequently reduced the ketone substrate through a stepwise transfer of hydrogen atoms to afford the (*R*)-alcohol (Scheme 11, **10f**). Authors noticed a hydrogen-bond between the carbonyl oxygen and the protonated amido moiety could favour the proton transfer while the transfer of the hydride could be a limiting step. It was also observed catalytic conditions implying more than 2 equivalents of base promoted the formation of the active mono(eneamido) species (**10c**) from the bis(eneamido) complex (**10b**) by preventing the formation of an inactive bis(amido) species (**10d**) through protonation and slow reduction of the mono(eneamido) complex (**10c**) (Scheme 11).

Following their mechanistic investigations, Morris et al. prepared a third generation of catalysts based on iron complexes (**11**) comprising amine imine diphosphine / PNNHP ligands which featured identical or different phosphine moieties with aryl and/or cyclohexyl substituents at phosphorus (Scheme 12) [78-81].
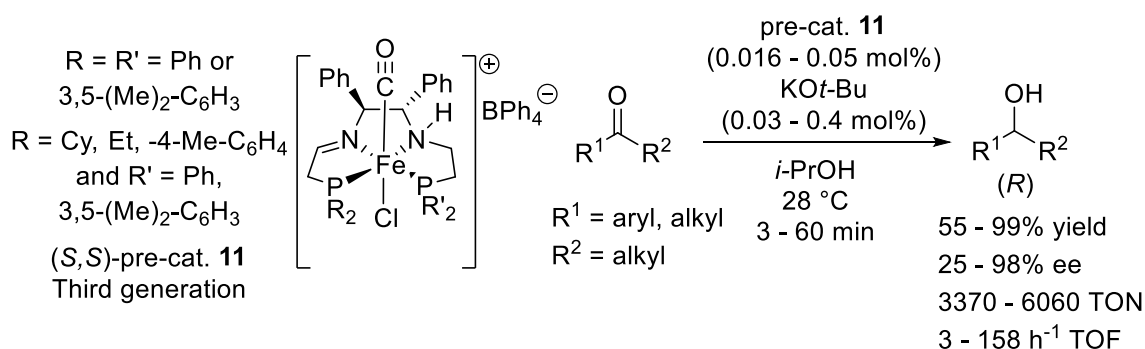
Scheme 12. ATH of ketones catalysed by iron complexes **11** based on chiral PNNHP ligands by Morris et al.

While cyclohexyl substituents at the phosphorus resulted in less active but sometimes more selective catalysts on specific substrates, the iron complexes with phenyl or xylyl substituents at the phosphorus were highly active and selective catalysts in the ATH of a large range of ketones (up to 6060 TON and 150 h^{-1} TOF, up to 98% ee). In a similar way to the second generation catalysts, the substitution by xylyl groups at the phosphorus atom led to the most selective catalyst, the highest activities being reached using phenyl groups. On the whole, a fine balance between steric and electronic properties was necessary to reach high activities and selectivities with this third generation catalyst. When these ketone ATH approached equilibrium, the decomposition of the catalyst or the racemization of the alcohol product were the main observed drawbacks.

The third generation of catalysts was also applied in ATH of aromatic ketones in aqueous biphasic conditions by Morris et al. (Scheme 13) [82]. Due to the oxygen sensitivity of the catalyst, the reactions were performed under an argon flow. MeTHF was used as co-solvent, NBu_4BF_4 or TWEEN80 as a surfactant and water and potassium formate as the proton and hydride sources respectively. By comparison to the corresponding homogeneous catalytic system, the catalysis was less effective but catalyst loadings remained low. Though less enantioselective (up to 76% ee), such iron based biphasic catalytic system had activities similar to ruthenium-based catalysts within identical biphasic conditions.
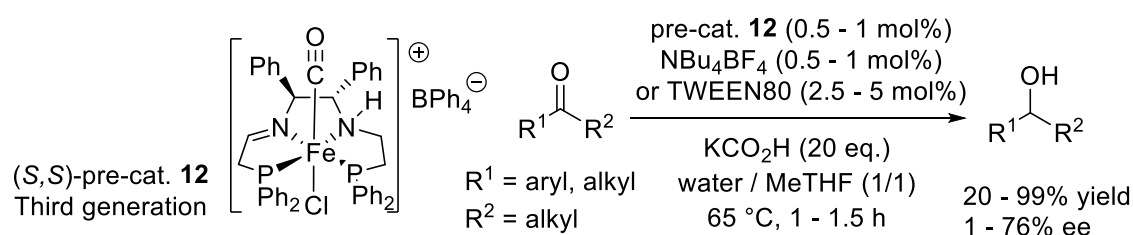
Scheme 13. ATH of ketones in water catalysed by iron complex **12** based on a chiral PNNHP ligand by Morris et al.

Worthy of note, Morris et al. prepared two *cis*-β iron(II) pre-catalysts (**13**) and (**14**) and applied them to the ATH of acetophenone (Scheme 14) [83]. They found an enantioinversion while applying complexes based either on a bis(amine)bisphosphine (**13**) or on a (amine)(imine)bisphosphine (**14**) ligand. By comparison to the third generation iron(II)

catalysts of C_2-symmetry, these species based on PNHNHP and PNNHP ligands were of C_1-symmetry. Though the activation of both complexes apparently resulted in similar diamido derivatives, the carbonyl ligand was directed upward or downward, i.e. on opposite sides of the plane of the PNNP ligand (Scheme 14). Hence, this led to two different hydride species and therefore to the (R) and (S) enantiomers of the 1-phenylethanol product. Though amine and imine based *cis*-β iron(II) complexes (**13**) and (**14**) displayed high and adjustable enantioselectivities, they were much less active than the third generation of iron(II) pre-catalysts (**11**).
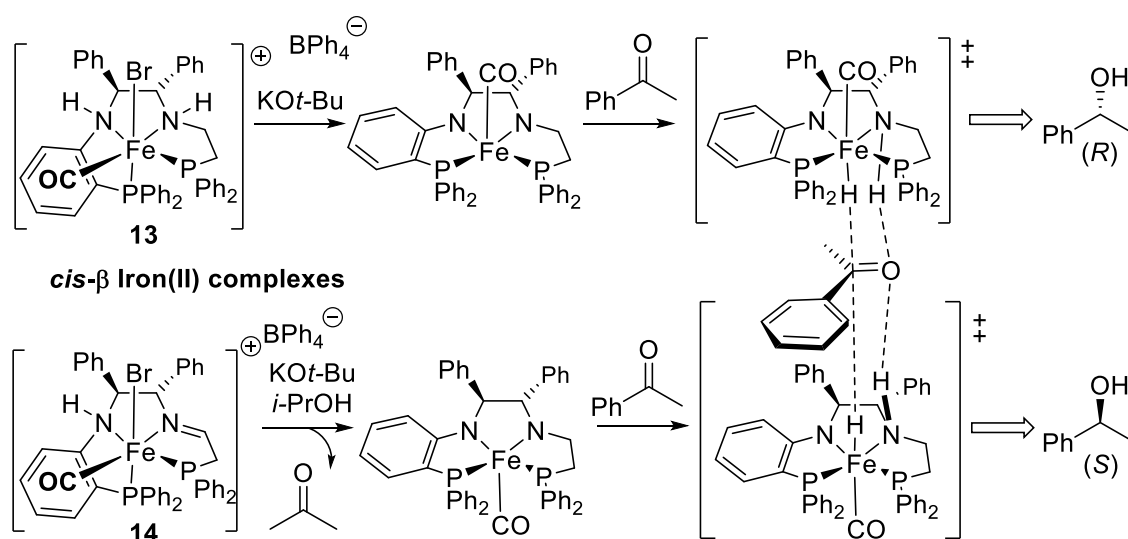
Scheme 14. Controled ATH of ketones catalysed by *cis* iron complexes **13** and **14** based on chiral PNHNHP and PNHNP ligands by Morris et al.

While studying their first generation of iron(II) pre-catalysts (**2**) in ATH of ketones and by performing advanced experiments and characterizations, Morris et al. showed the active species were superparamagnetic chiral iron(0) nanoparticles of around 4.5 nm in diameter [84-86]. Thanks to kinetic analyses, they observed an induction period which was credited to the activation and therefore the reduction of the iron(II) precatalyst with base and isopropanol. However, the involvement of minor amounts of an iron homogeneous catalyst which was produced in parallel could not be ruled out. By comparison, the second generation of iron(II) pre-catalysts (**9**), (**10a**), (**10g**), (**10i**) and (**10j**) remained homogeneous but Morris et al. evidenced a degradation pathway related to the bifunctional property of the PNNP ligand [86]. Indeed, according to experiments, analyses and calculations, they observed and characterized

deactivated species: a partially reduced and racemized complex (**10h**) along with 2 minor iron-hydride compounds (Scheme 15).
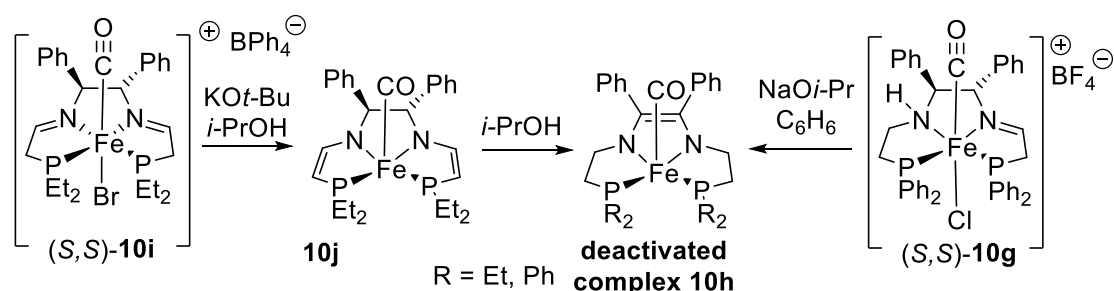

Scheme 15. Deactivation of iron complexes **10g** and **10i** based on PNHNP and PNNP ligands by Morris et al.

Starting from 2014, Mezzetti et al. reported on the synthesis and the characterization of diamagnetic chiral iron(II) complexes based on chiral N_2P_2 macrocyclic ligands and isonitriles as ancillary ligands (Scheme 16) [87-90]. Application of the resulting Λ-*cis*-β iron(II) complexes (**15**) to the ATH of a broad scope of ketones provided the corresponding alcohols in good to high yields (62–99%) and enantioselectivities (24-99% ee) but alkylated substrates were more challenging than aryl,alkyl-ketones. According to these results, Mezzetti catalysts had similar performances than Morris second generation iron(II) catalysts (**9**). Preliminary mechanistic studies highlighted the pre-catalyst required an activation in order to be active in transfer hydrogenation, two imine functions of the pre-catalyst being reduced to amines along with the partial hydrogenation of one isonitrile ligand. No free macrocyclic ligand and therefore no catalyst decomposition were observed along this process even upon addition of an additionnal ligand and reducing agent like triphenylphosphine.
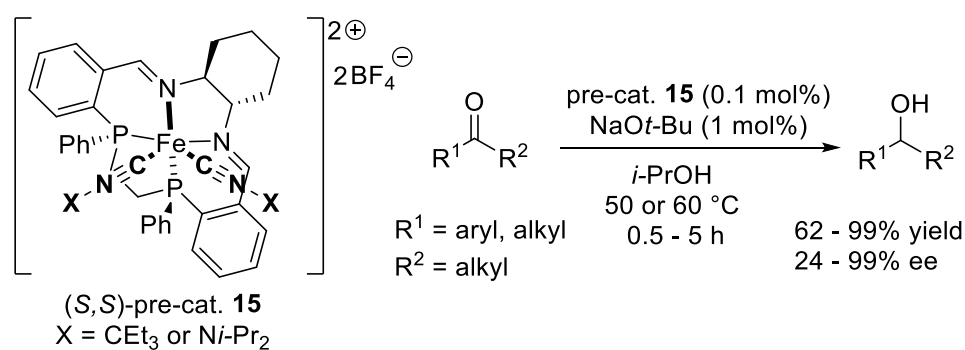
Scheme 16. ATH of ketones catalysed by iron complexes **15** based on a chiral PNNP macrocyclic ligand by Mezzetti et al.

In two further and consecutive publications, Mezzetti et al. reported the synthesis, characterization and reactivity of improved iron(II) pre-catalysts (**16a**) and (**16c**) based on a propane-1,3-diyl-bridged (NH)$_2$P$_2$ macrocycle and isonitriles as ancillary ligands (Scheme 17) [91-92]. First, they demonstrated the addition of a methylene unit and the change of initial imine groups (Scheme 16) for amines into the macrocycle significantly increased the activity (up to 99% yield) and selectivity (up to 99% ee) of the catalysts for the ATH of ketones (Scheme 17) [91].
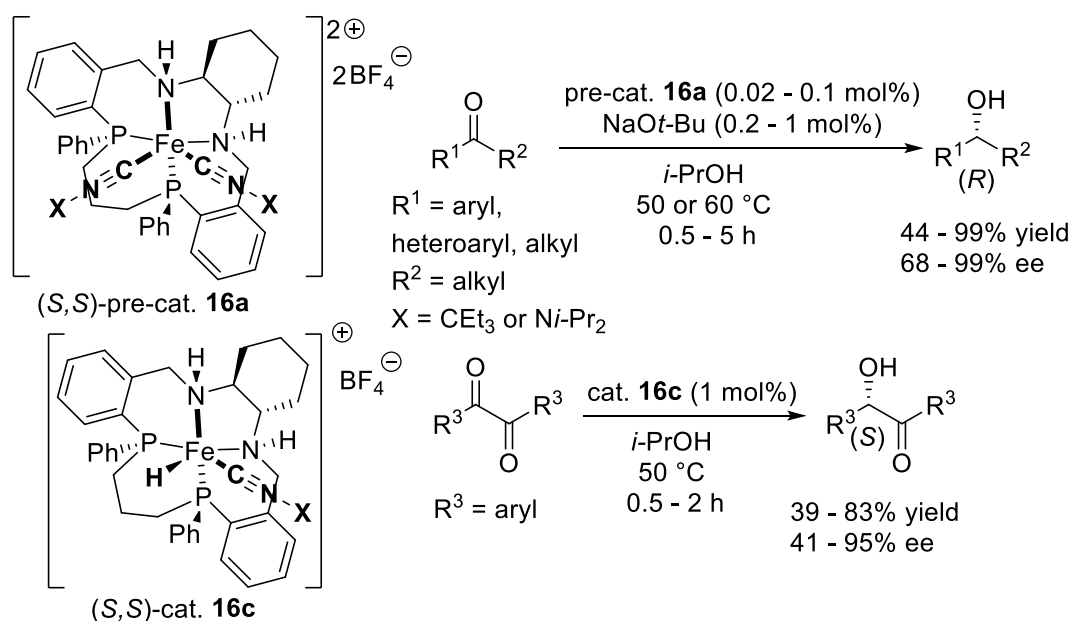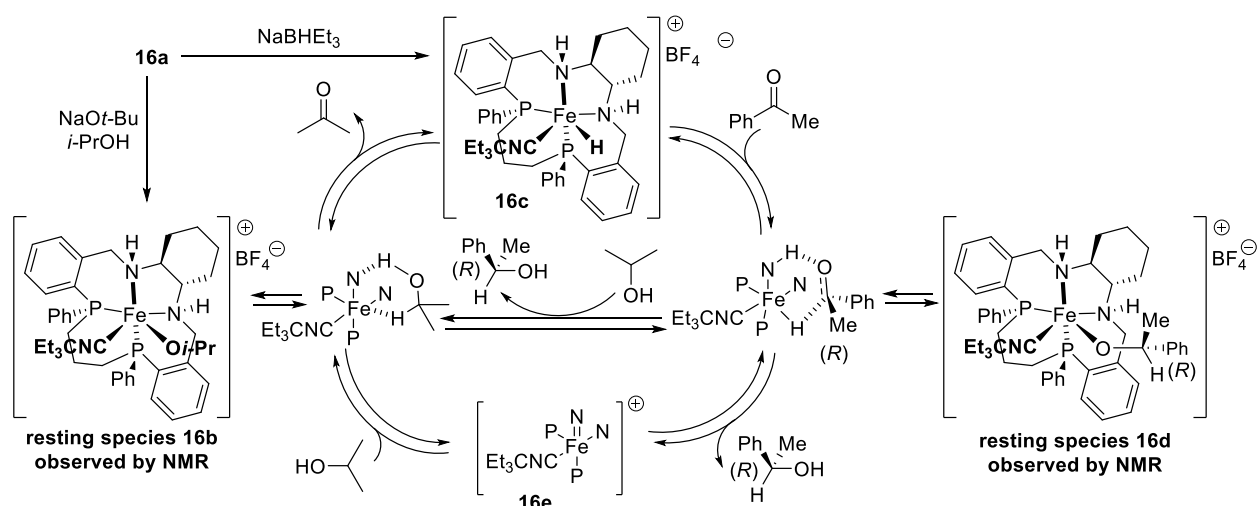

Scheme 17. ATH of ketones and 1,2-diketones catalysed by iron complexes **16a** and **16c** based on a PNHNHP macrocyclic ligand by Mezzetti et al.

The related *cis*-β iron(II) hydride complex (**16c**) was subsequently prepared and applied as catalyst for the hydrogenation of ketones. Though this hydride species could operate under base free conditions, it was less active, the use of a base being required for a high catalytic activity. Nevertheless, such ATH under base free conditions allowed the first selective hemireduction of 1,2-diketones like benzil within average to high yields (39-83%) and enantioselectivities (41-95% ee) [92].

Through experimental, analytical and theoretical studies, Mezzeti et al. studied in more detail their iron catalysed ATH and proposed a catalytic cycle (Scheme 18) [93]. The first step which is turnover determining implied the formation of an iron hydride complex (**16c**) by proton elimination from 2-propoxide adduct (**16b**) and release of acetone. Afterwards, a bifunctional mechanism allowed the insertion of acetophenone into the Fe-H bond. The neighbouring *syn-*

NH interacted with the substrate through hydrogen bonding with the carbonyl function. This enabled a stepwise transfer of the hydride and the proton of the amine, the hydride transfer being the enantiodetermining step. Afterwards, the adduct gathering the iron catalyst and the 1-phenylethanol product could be protonated thanks to the presence of 2-propanol. This led either to transient iron(II) species H-bonded to 2-propoxide ion (**16b**) and (**16d**), or to a transient iron mono-amido complex (**16e**) which could be generated by deprotonation of an amine group from an iron(II) complex based on $(NH)_2P_2$ macrocycle and two isonitriles. The subsequent formation of the iron hydride complex (**16c**) from the iron amido complex proceeded by reaction with 2-propanol. In addition, authors observed by NMR the presence of two off-cycle iron(II) species: a 1-phenylethanolato complex (**16d**) and 2-propoxo complex (**16b**). However, the excess of 2-propanol used as solvent pushed the equilibrium privileging the formations of the in-cycle iron species and the reaction product. Finally, the stereochemical model applied in the calculations reproduced the high enantioselectivity experimentally observed.

Scheme 18. Mechanism of ATH of ketones catalysed by an iron complex **16a** based on a chiral PNHNHP macrocyclic ligand by Mezzetti et al.

Following their previous studies in this field [60], Gao et al. reported the ATH of ketones through the use of an in-situ prepared catalyst by combining a chiral $P_2(NH)_4$ macrocyclic ligand (**L3**) with iron cluster $Fe_3(CO)_{12}$ and additives (Scheme 19) [94]. The ATH of a range of ketones proceeded in high conversions (64-98%) and enantioselectivities (91-99% ee) at a rather low catalyst loading. An isolated bimetallic complex combining this macrocyclic ligand and two $Fe(CO)_4$ fragments proved to be a much less active and selective catalyst.
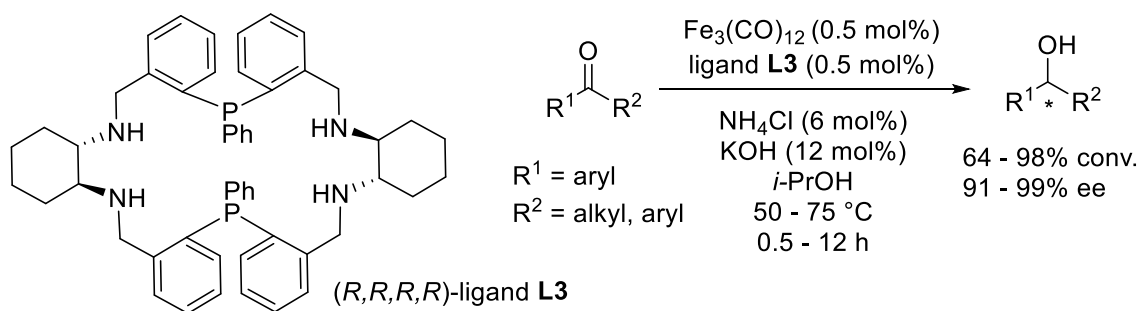
Scheme 19. ATH of ketones catalysed by iron complexes based on a PNHNHPNHNH macrocyclic ligand **L3** by Gao et al.

3.2. Mn based catalysts.

In 2017, Kirchner et al. reported the synthesis of a manganese(I) complex based on an unsymmetrical chiral PNP′ pincer ligands comprising a planar chiral Ferrocene and a chiral aliphatic amine (Scheme 20) [95].
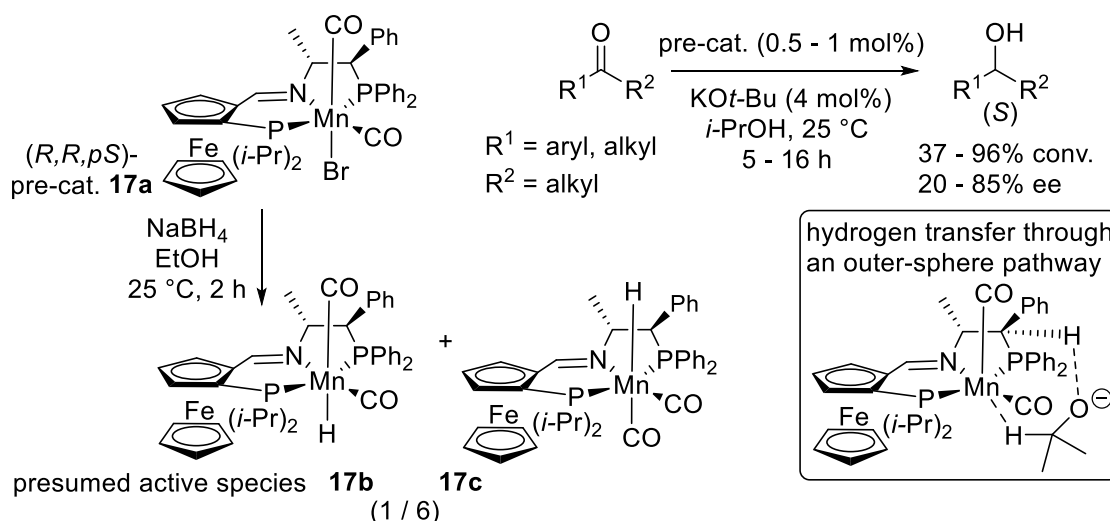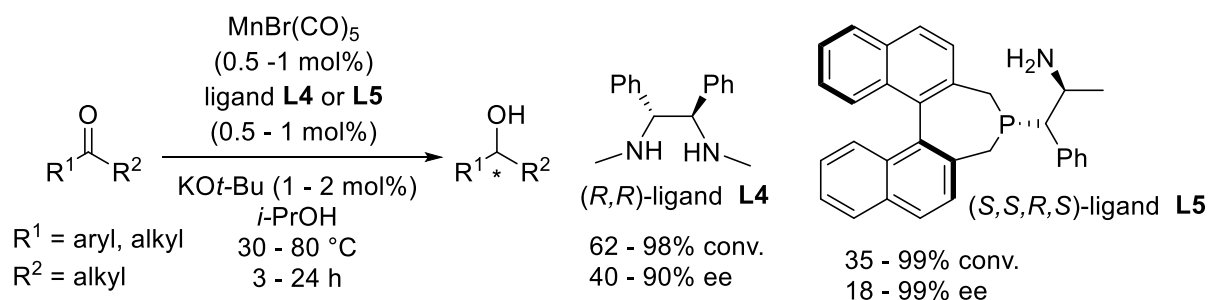

Scheme 20. ATH of ketones catalysed by manganese(I) complex (**17a**) based on a chiral PNP ligand by Kirchner et al.

The isolated bromide manganese(I) complex (**17a**) catalysed the ATH of ketones at reasonable catalyst loadings with average to high conversions (37-96%) and low to good enantioselectivities (20-85% ee). The reaction of the bromide manganese(I) complex (**17a**) with NaBH₄ resulted in a mixture of two manganese(I) hydride complexes (**17b**) and (**17c**) which led to catalytic results similar to those for the bromide complex (**17a**) (Scheme 20). According to experiments and calculations, the pre-catalyst was first dehalogenated and the resulting cationic species interacted with an isopropoxide through hydrogen bonding between the oxygen

atom and the acidic CH bond adjacent to the phosphine moiety (Scheme 20). This allowed an outer-sphere hydrogen transfer and therefore the formation of the hydride species. Due to steric hindrance and to a hydrogen bonding between the ligand and the carbonyl of the ketone substrate, the minor manganese(I) hydride (**17b**) was the single active species leading to (*S*)-alcohols.

In 2018, Sortais et al. studied the ATH of a broad scope of ketones by performing a wide screening of chiral amine ligands. They found the combination of dimethylated DPEN (**L4**), MnBrCO$_5$ and KO*t*-Bu base led to an effective catalyst (Scheme 21) [96]. At 80°C, conversions were good to high (62-98%) and enantioselectivities average to high (40-90% ee). Afterwards, these authors screened various bidentate aminophosphine ligands and found the combination of ligand (**L5**) bearing a bulky binepine moiety on the phosphorus atom with MnBr(CO)$_5$ and KO*t*-Bu allowed the ATH of ketones with high ees (up to 99% ee) at the exception of dialkylketones (Scheme 21) [97]. Except for sterically hindered substrates, most of the reactions proceeded with high conversions at 30 °C (up to 99%).

Scheme 21. ATH of ketones catalysed by manganese(I) complexes based on chiral NHNH **L4** and PNH$_2$ **L5** bidentate ligands by Sortais et al.

After their successful development of three generations of iron(II) catalysts, Morris et al. studied also manganese(I) catalysts. Among the several complexes prepared from PNHNH$_2$ ligands, a *syn-mer* borohydride complex (**18a**) and a pentavalent amido complex (**18b**) showed interesting catalytic activities in the ATH of a range of ketones without the use of a base (Scheme 22) [98]. In spite of high conversions (69-99%) and good chemoselectivity, enantioselectivities were low to average (9-53% ee). A catalytic cycle was proposed on the basis of experimental and analytical data. The borohydride complex (**18a**) led first to the *syn* NH hydride species (**18c**). Afterwards, the transfer of a hydride and a proton to the ketone substrate proceeded through a concerted or stepwise mechanism releasing the (*R*)-alcohol product and forming a pentavalent amido complex (**18d**). The latter reacted then with 2-

propanol through an outer-sphere, six-membered transition state which allowed the transfers of proton and hydride and therefore the reformation of *syn*-NH hydride complex (**18c**) and residual acetone. Furthermore, the amido complex (**18d**) was also prepared under basic conditions by dehalogenation and subsequent deprotonation of bromo precursor (**18b**).
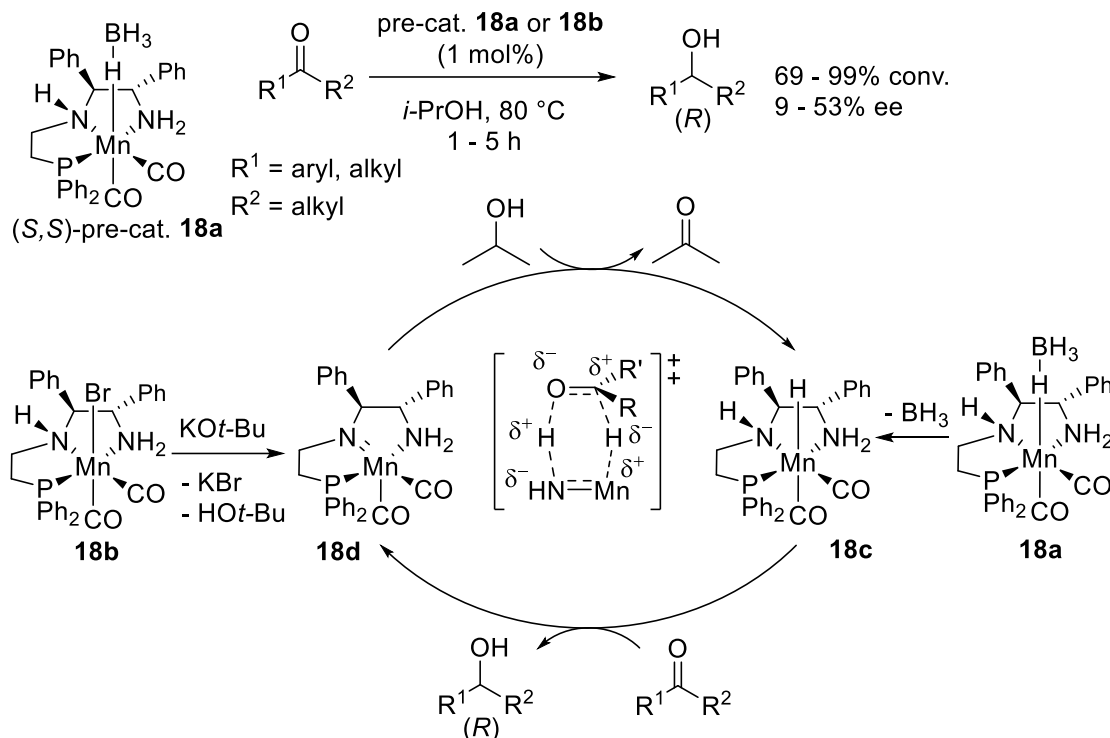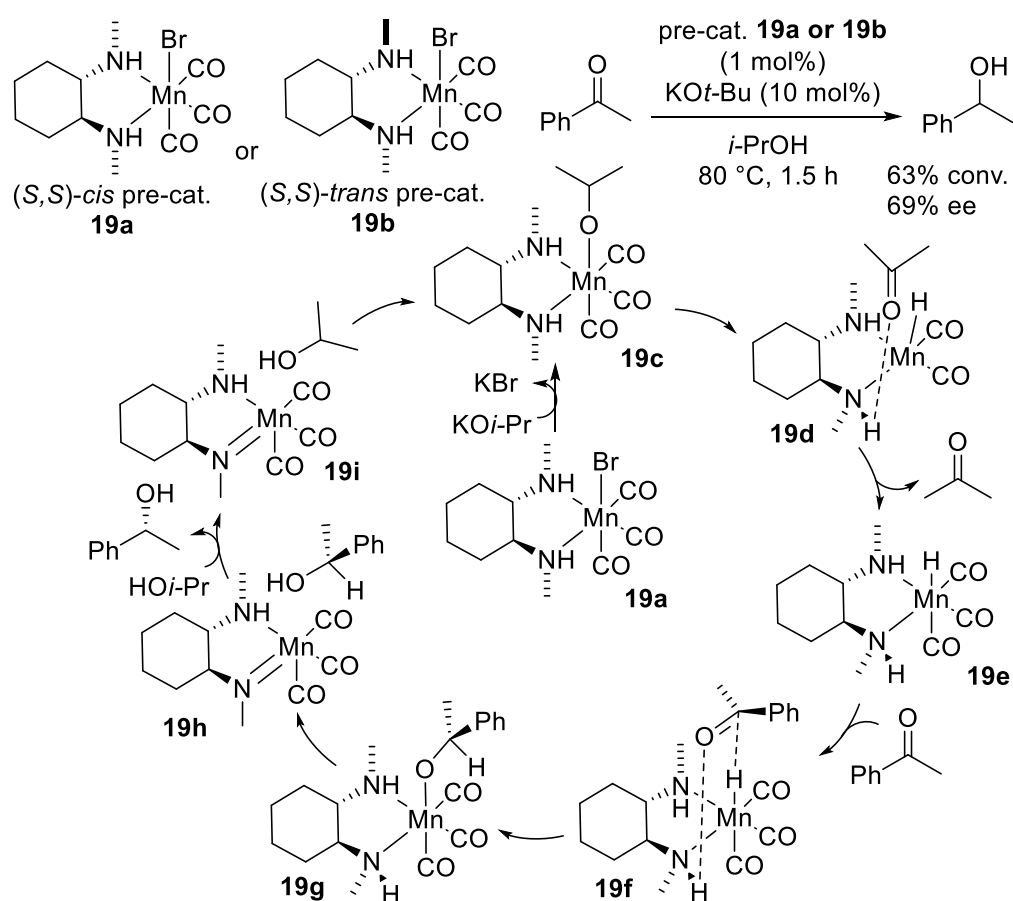

Scheme 22. ATH of ketones catalysed by manganese(I) complexes **18a** or **18b** based on a chiral PNHNH$_2$ ligand by Morris et al.

In 2019, Beller et al. reported an alternative to the use of chiral phosphorus ligands thanks to a large screening of ligands, manganese precursors and reaction conditions (Scheme 23) [99]. Indeed, the one-pot combination of a C_2-symmeric phenyl-substituted *N,N'*-bis(2-hydroxyethyl)oxamides (**L6**) with MnBrCO$_5$ and KO*t*-Bu base provided an active catalyst for the ATH of a series of ketones. Yields (23-99%) and enantioselectivities (19-93% ee) were low to high, aliphatic ketones giving the best results.
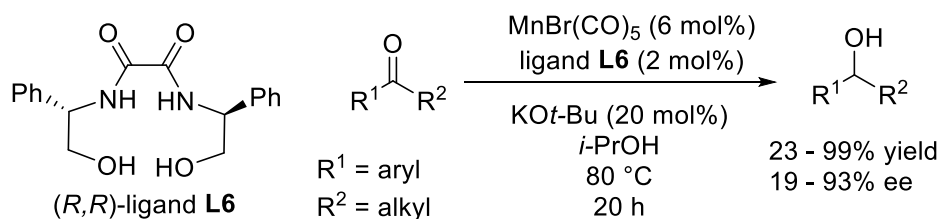
Scheme 23. ATH of ketones catalysed by a combination of MnBr(CO)$_5$ and a OHNHNHOH ligand **L6** by Beller et al.

In parallel, Pidko et al. tested several chiral manganese(I)−diamine complexes as catalysts for the ATH of acetophenone (Scheme 24) [100]. *Cis-* and *trans*-complexes (**19a**) and (**19b**) based on chiral diaminocyclohexane were the most effective with similar conversions (63%) and enantioselectivities (69% ee).
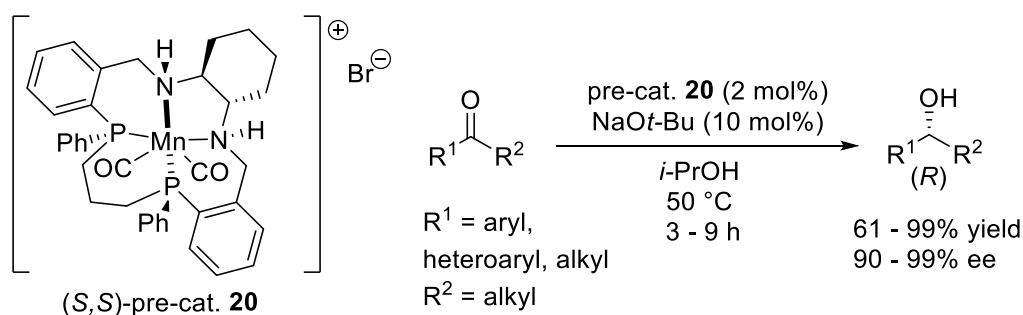

Scheme 24. ATH of ketones catalysed by manganese(I) complexes **19a** or **19b** based on a chiral NHNH bidentate ligand by Pidko et al.

An increase of the catalyst steric hindrance failed in improving the enantioselectivity while preserving a good activity. Theoretical calculations, kinetic and experimental investigations were performed to study the reaction mechanism (Scheme 24). The catalyst resting state was a manganese-isopropoxide complex (**19c**) formed upon activation by debromination and activation of 2-propanol. A manganese-hydride complex (**19e**) was then formed by β-Hydride elimination of the isoproxide and release of acetone from intermediate (**19d**). Afterwards, an adduct (**19f**) is formed with the acetophenone through hydrogen bonding between the substrate carbonyl and the NH from the diaminocyclohexane ligand. This allowed the

enantiodetermining hydride transfer and the formation of a manganese-alkoxide resting species (**19g**). Release of 1-phenylethanol product proceeded by deprotonation of a ligand NH group and generation of manganese-amido intermediates (**19h**) and (**19i**) which reacted readily with 2-propanol and regenerate the manganese-isopropoxide complex (**19c**). According to the authors, the catalyst optimization appeared challenging as different pre-catalysts led to same intermediates and therefore to an identical catalytic outcome.

Following their work on iron chiral catalysts, Mezzetti et al. recently prepared manganese(I) complex (**20**) based on a macromolecular PNHNHP chiral ligand (Scheme 25) [101]. The application to the ATH of a broad scope of ketones led to alcohols in very high yields (61-99%) and enantioselectivities (90-99% ee) with excellent chemoselectivity and minor limitations for hindered substrates. Preliminary calculations highlighted the high enantioselection resulted from attractive CH–π interactions between the alkyl group of ketone substrate and one phosphine phenyl ring of the catalyst.

Scheme 25. ATH of ketones catalysed by a manganese(I) complex **20** based on a chiral PNHNHP macrocyclic ligand by Mezzetti et al.

3.3. Cobalt and nickel based catalysts.

Following their investigations on iron catalysts, Gao et al. reported a nickel catalyst based on a polydentate ligand of PNO type (**L7**) based on (*R*)-phenylglycinol (Scheme 26) [102]. Application to the ATH of ketones led to alcohols in average to high conversions (51-98%) and enantioselectivities (60-84% ee), the reactions operating with higher loadings of catalyst and base than the related iron catalysts.
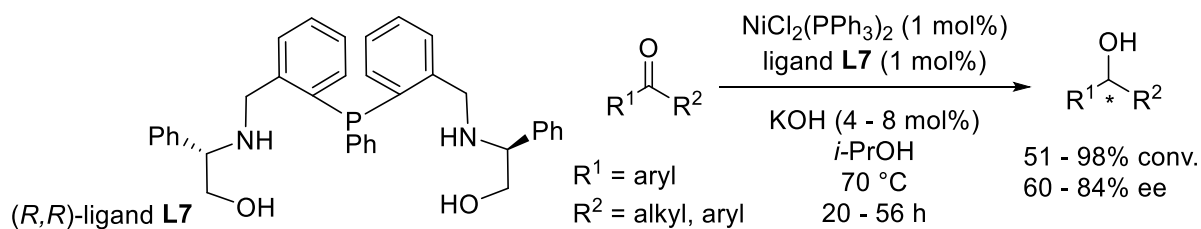
Scheme 26. ATH of ketones catalysed by a combination of $NiCl_2(PPh_3)_2$ and a polydentate ligand of PNO type **L7** by Gao et al.

In parallel, Gao et al. studied also cobalt catalysts for the ATH of ketones by combining tetradentate PNHNHP (**L1**) and PNNP (**L2**) ligands with cobalt precursors [59,60]. The use of a PNHNHP ligand (**L1**) resulted in the most active catalyst (Scheme 27) but, by comparison to its iron counterpart, such cobalt catalyst exhibited a lower activity requiring higher temperatures, longer reaction times and higher amounts of base. The conversions were low to high (24-99%) depending on the substrate and enantioselectivities were low to average (6-63% ee).
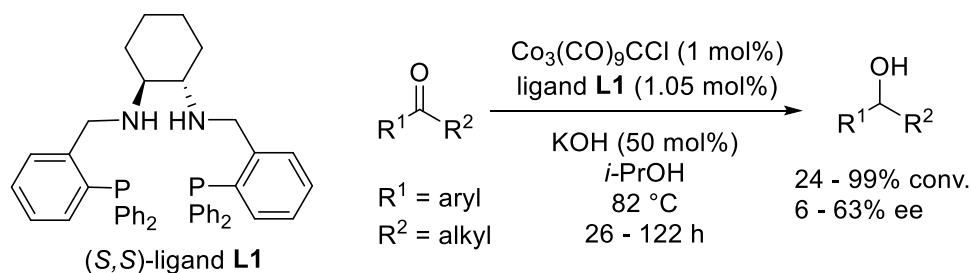

Scheme 27. ATH of ketones catalysed by a combination of $Co_3(CO)_9CCl$ and a PNHNHP ligand **L1** by Gao et al.

4. Asymmetric hydrogenation.

### 4.1.1. Chiral Knölker-type complexes.

In 2011, Berkessel et al. reported the synthesis under photolytic conditions of several iron(II) cyclopentadienone dicarbonyl complexes coordinated to a chiral phosphoramidite ligand (Scheme 28) [103]. Once decarbonylated upon irradiation, complex (**21**) was an active catalyst for the AH of acetophenone but the enantioselectivity was modest (31% ee). A ^{1}H NMR study highlighted the formation of several active hydride complexes which were detrimental in highly enantioselective AH. Indeed, the photolytic dissociation of a carbonyl ligand and the subsequent hydrogen uptake generated a stereogenic center at iron and therefore resulted in two

diasteromeric hydride complexes with low selectivity (6/4 ratio). Furthermore, the dissociation of the phosphoramidite ligand prior to H_2 uptake led to the formation of a minor achiral hydride.
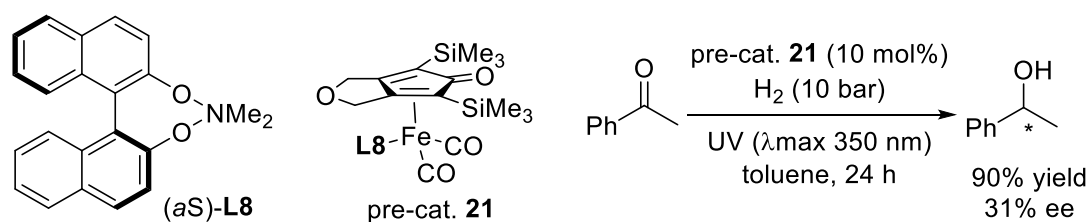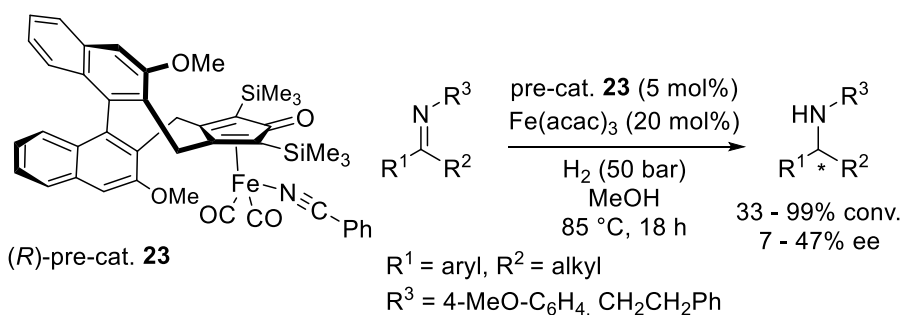

Scheme 28. AH of acetophenone catalysed by chiral iron(II) cyclopentadienone dicarbonyl complex **21** by Berkessel et al.

In 2015, Gennari, Pignataro, Lefort, de Vries et al. developed a family of chiral (cyclopentadienone)iron complexes (**22**) featuring a (R)-binaphtyl backbone with various substituents on the 3,3'-positions (Scheme 29) [104,105]. Upon activation by decarbonylation with Me_3NO, these complexes catalysed the AH of a range of aryl,alkyl- and dialkyl-ketones. At the exception of dialkyl-ketones which remained challenging, the conversions were fair to quantitative and enantioselectivities were average to rather high (up to 77% ee). The catalyst bearing methoxy substituents on the 3,3'-positions of the binaphtyl backbone was the most active and selective.
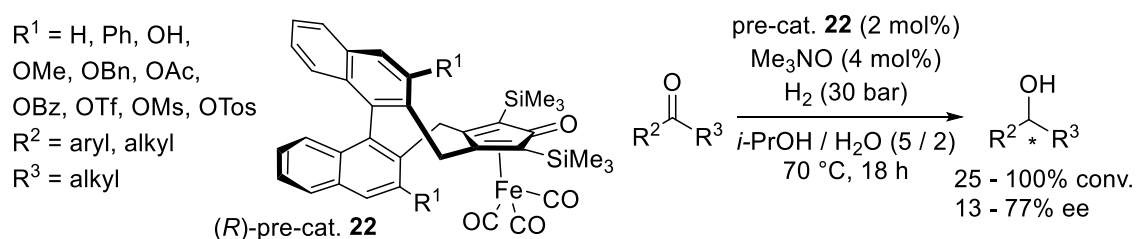

Scheme 29. AH of ketones catalysed by chiral iron(II) cyclopentadienone dicarbonyl complexes **22** by Gennari et al.

Recently, Gennari, Pignataro et al. pursued the development of their chiral (cyclopentadienone)iron complexes featuring a (R)-binaphtyl backbone by changing a carbonyl ligand for a benzonitrile (Scheme 30) [106]. The pre-catalyst (**23**) was decoordinated under reflux in methanol and led to an active catalyst for the AH of imines provided the Lewis acid $Fe(acac)_3$ was used in order to activate the imine reagents. Yields were low to high (33-99%) and enantioselectivities were low to average (7-47% ee). Interestingly, the pre-catalyst (**23**) was also active for the reductive-amination of ketones.

Scheme 30. AH of imines catalysed by chiral iron(II) cyclopentadienone dicarbonyl complex **23** by Gennari et al.
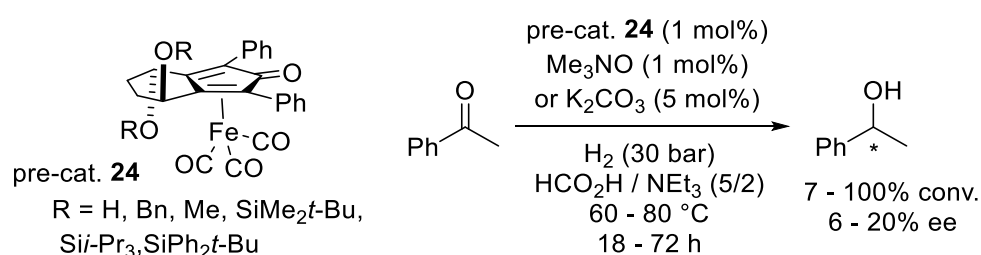
Scheme 31. AH of acetophenone catalysed by chiral iron(II) cyclopentadienone tricarbonyl complexes **24** by Wills et al.

In 2016, Wills et all. described a series of enantiomerically-pure iron tricarbonyl cyclopentadienone complexes (**24**) and investigated the AH of acetophenone by combining hydrogenation to transfer hydrogenation (Scheme 31) [67]. Though all pre-catalysts provided active species once decarbonylated, the enantiomeric excesses were low (6-20% ee) but the catalysts bearing the bulkier silicon groups were the most selective. Furthermore, the derivatization of the catalysts by decarbonylation and coordination to a Monophos phosphoramidite ligand resulted in poorly active catalysts.

In parallel, Renaud, Ward et al. reported on the synthesis of biotinylated (cyclopentadienone)iron tricarbonyl complex (**25**), the in-situ generation of the corresponding streptavidin conjugates and their application in AH of an imine and some ketones (Scheme 32) [107]. Though the conversions (12 or 26%) and enantioselectivities (20 or 34% ee) were low, one of the resulting artificial iron hydrogenases proved to be an active catalyst for the reduction of an activated ketone, enantiomeric excess remaining low (9% ee).
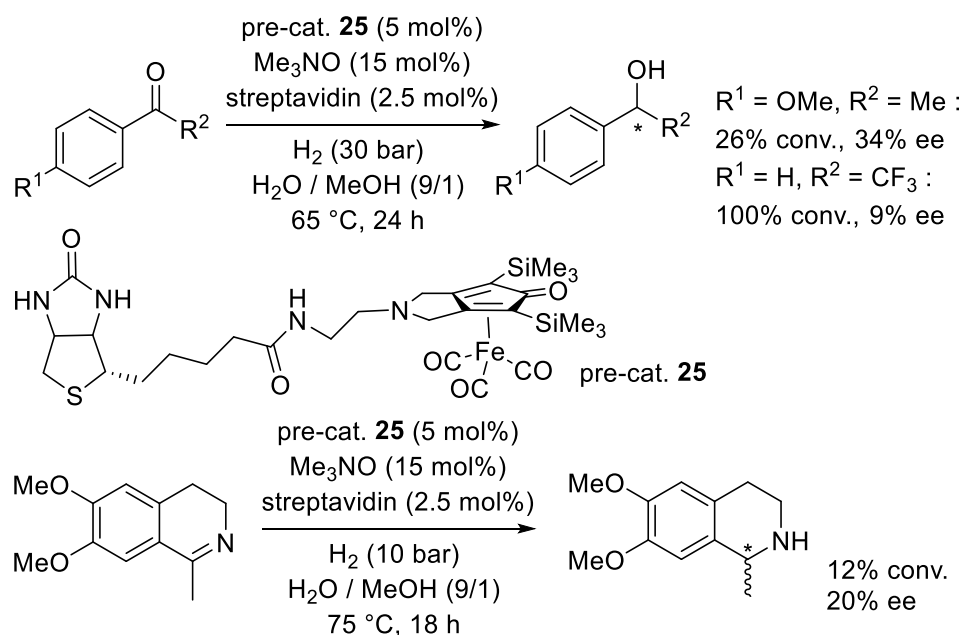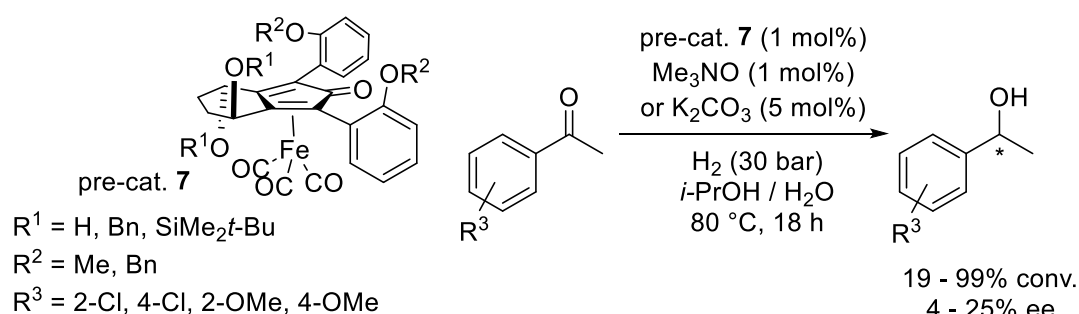
Scheme 32. AH of ketones and imines catalysed by an iron(II) cyclopentadienone tricarbonyl complex **25** by Renaud, Ward et al.

Afterwards, Benaglia et al. reported on the application of cyclopentadienone-based iron complex (**26**) to catalyse the diastereoselective hydrogenation of enantiopure imines (Scheme 33) [108]. At the exception of electron poor imines, all enantiopure substrates led to amine products in fair yields and high diastereomeric excesses (up to 96% de). A theoretical study underlined the transfer of the hydride from the iron to the imine carbon occured when the proton transfer from the hydroxyl group of the hydrogenated catalyst to the imine nitrogen had almost completely occurred in a concerted but asynchronous mechanism. Furthermore, the hydride transfer operated onto the *Re*-face of the (1*S'*)-imines due to transition states at lower energy.
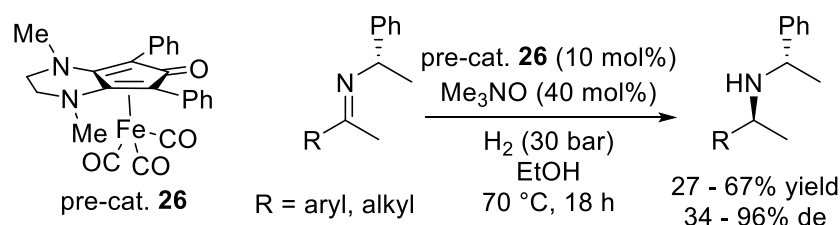

Scheme 33. AH of enantiopure imines catalysed by an iron(II) cyclopentadienone tricarbonyl complex **26** by Bennaglia et al.

Following their previous investigations, Wills et al. studied a series of cyclopentadienone iron tricarbonyl complexes (**7**) as pre-catalysts for AH of aryl-ketones (Scheme 34) [109]. Among the prepared complexes, it was noticed a symmetrical substitution pattern around the central CO bond by bulky anisole-type groups had a positive impact on the asymmetric induction. Though complexes (**7**) proved to be effective pre-catalysts for the reduction of acetophenone derivatives, the resulting alcohols were formed in low ees (4-25% ee). Catalyst bearing only benzylether groups was the most effective and selective. Substitution by pyridyl of the alcohol groups from the cyclohexyl backbone failed in affording any asymmetric induction in the hydrogenation of acetophenone.

Scheme 34. AH of ketones catalysed by chiral iron(II) cyclopentadienone tricarbonyl complexes **7** by Wills et al.
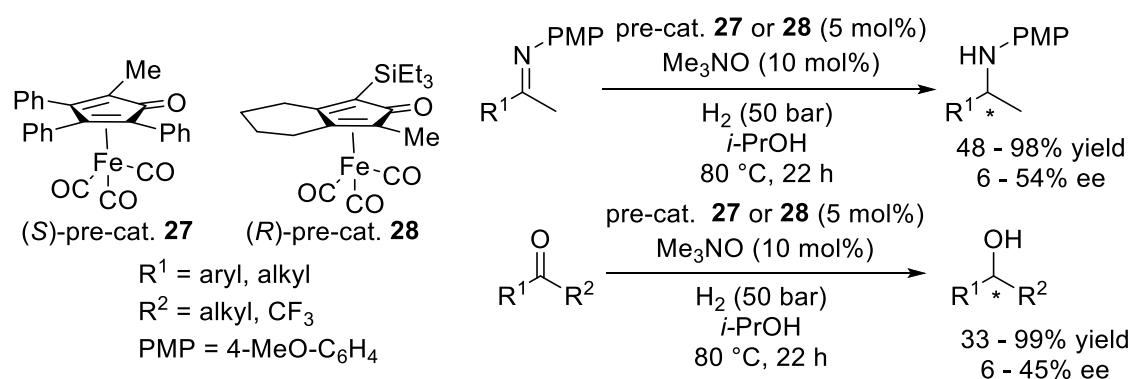
Scheme 35. AH of ketones and imines catalysed by chiral iron(II) cyclopentadienone tricarbonyl complexes **27** and **28** by Gennari et al.

In 2019, Gennari, Pignataro et al. synthesized planar chiral (cyclopentadienone)iron complexes (**27**) and (**28**) starting from readily accessible achiral materials and separeting the enantiomers by preparative CSP HPLC (Scheme 35) [110]. The pre-catalysts (**27**) and (**28**) were applied to the AH of ketones and ketimines and the resulting alcohols and amines were obtained in fair to high yields (33-99%) with low to average enantioselectivities (up to 54% ee for amines

and up to 45% ee for alcohols). The silylated pre-catalyst was better reducing the ketones than the imines with slightly higher enantiomeric excesses.

The chiral Knölker-type complexes (**8**) applied in ATH of ketones by De Wildeman et al. were applied in AH of a range of ketones bearing alkyl and aryl or heteroaryl substituents (Scheme 36) [68]. The resulting alcohols were obtained with fair to high conversions and low to good enantioselectivities, some being among the highest obtained using chiral Knölker-type catalysts. NMR studies confirmed the asymmetric structures of the complexes and theoretical calculations highlighted on the structural conformations of the ligands.

n = 0 or 1
R^1 = Me, Ph
R^2 = Sii-Pr$_3$, SiPh$_2$$t$-Bu
R^3 = aryl, heteroaryl
R^4 = Me, Et

pre-cat. **8**

pre-cat. **8** (1 mol%)
Me$_3$NO (3 mol%)
H$_2$ (50 bar)
i-PrOH
60 °C, 24 h

32 - 99% conv.
14 - 70% ee
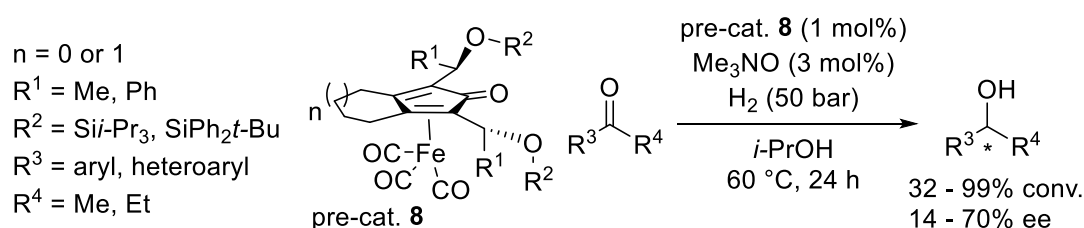
Scheme 36. AH of ketones catalysed by chiral iron(II) cyclopentadienone tricarbonyl complexes **8** by De Wildeman et al.

In a seminal publication, Beller et al. combined achiral iron Knölker hydride complex (**29**) to (*S*)-TRIP Brønsted acid (**31**) to catalyse the enantioselective hydrogenation of ketimines to secondary amines with high yields (up to 94%) and enantioselectivities (up to 98% ee) (Scheme 37) [111]. According to an in-situ ^{31}P NMR study, both catalysts cooperated in a bifunctional way. The (*S*)-TRIP Brønsted acid (**31**) protonated first the imine reagent. The resulting chiral zwiterrion was then hydrogenated by the achiral iron Knölker catalyst (**29**) to afford the corresponding amine, the (*S*)-TRIP Brønsted acid (**31**) and complex (**30**) which could further activate hydrogen gas.

Beller et al. subsequently applied their catalytic system to the AH of quinoxalines and benzoxazines (Scheme 37) [112]. The reduced heterocycles were obtained in good to high yields (67-97%) and average to high enantioselectivities (58-90% ee). Interestingly, they also reported the direct synthesis of chiral tetrahydroquinoxalines through reductive amination.
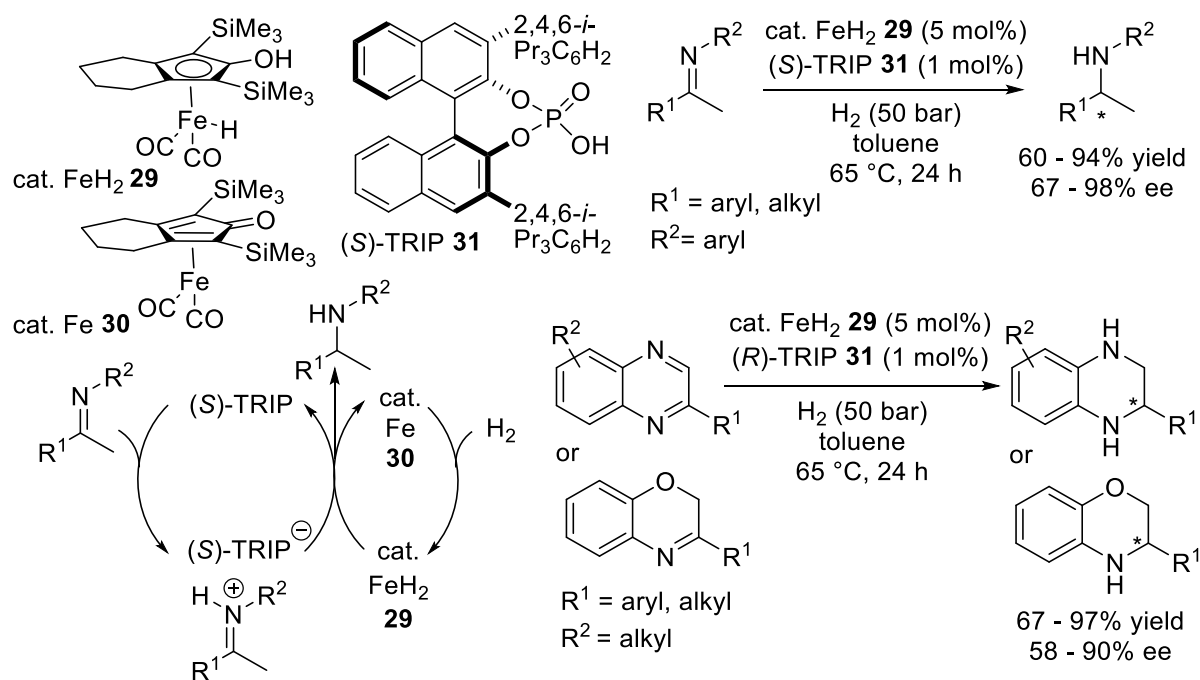
Scheme 37. AH of imines catalysed by a combination of iron(II) cyclopentadienone dicarbonyl hydride complex **29** and (*S*)-TRIP Brønsted acid **31** by Beller et al.

Later on, Beller et al. applied their catalytic system to enantioselective reductive hydroaminations. In a sequential way, they performed a gold catalysed hydroamination of terminal alkynes with anilines followed by the asymmetric hydrogenation of the resulting imines (Scheme 38) [113]. The related secondary amines were obtained in good to high yields (71-96%) and enantioselectivities (67-94% ee).
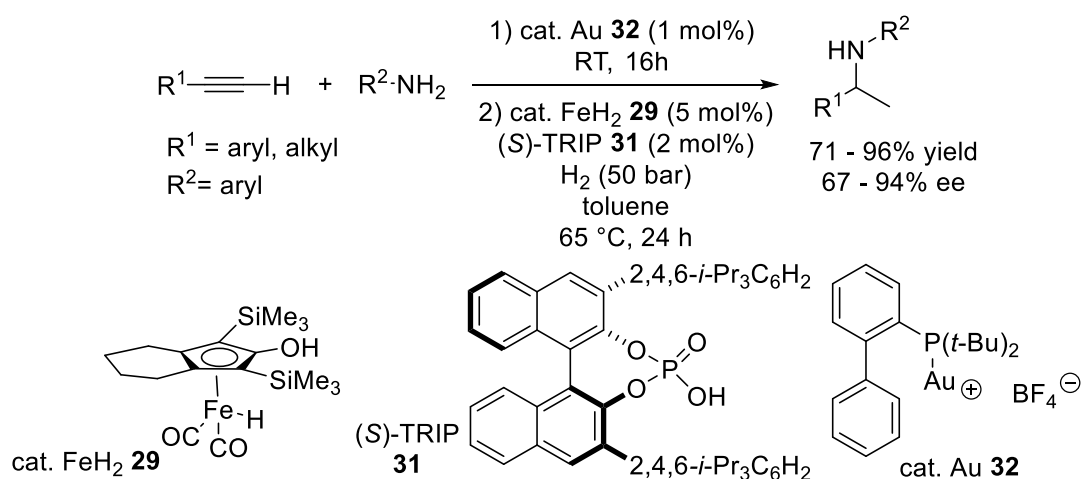
Scheme 38. Asymmetric sequential hydroamination and hydrogenation catalysed by combining achiral cationic Gold(I) complex **32** with achiral iron(II) cyclopentadienone dicarbonyl hydride complex **29** and (*S*)-TRIP Brønsted acid **31** by Beller et al.
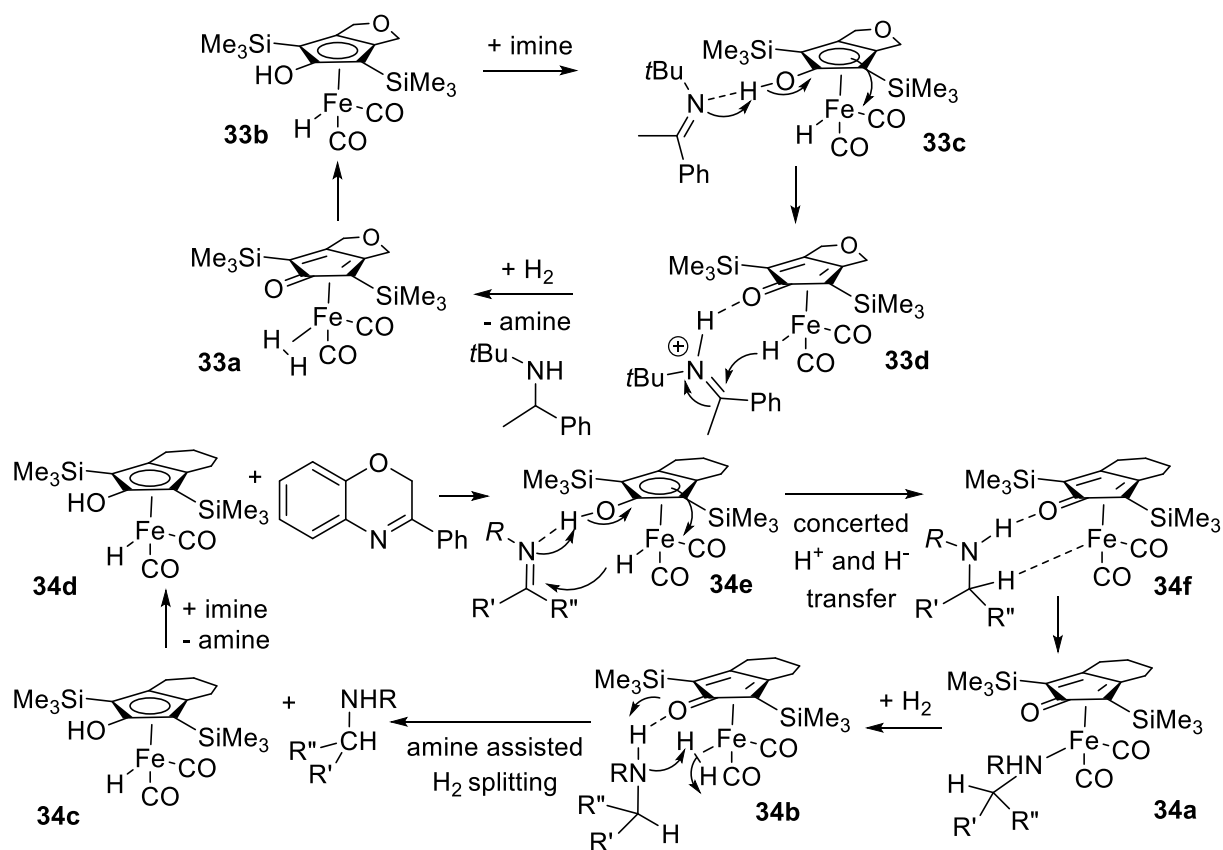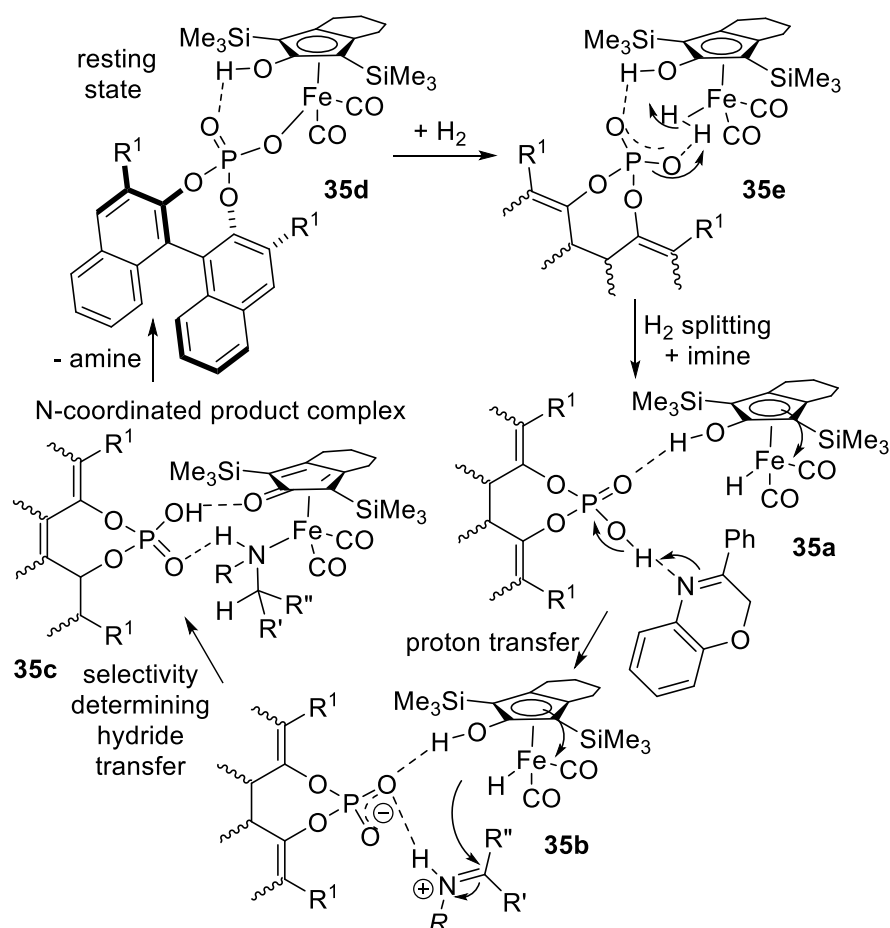
Scheme 39. Mechanism of the AH of imines and benzoxazines catalysed by an iron(II) cyclopentadienone dicarbonyl hydride complex by Berkessel et al. (top) and Hopmann et al. (bottom).

According to theoretical and experimental studies, the mechanism of imine hydrogenation using a Knölker's complex as catalyst without acid depends of the substrate (Scheme 39) [114,115]. At first, the Knölker complex featuring an iron(II) hydride and an hydroxy group on the cyclopentadienyl ligand was found the active species for hydrogenation. A proposal by von der Höh and Berkessel suggested the hydrogenation of an acyclic imine should occur through stepwise proton and hydride transfer with a coordinatively unsaturated iron(0) complex (**33a**) as initial species and complexes (**33c**) and (**33d**) as intermediates (Scheme 39, top) [114]. Coordination of H_2 to the iron center was followed by a proton transfer from H_2 to the cyclopentadienone ligand to afford the active hydride complex (**33b**).

For a cyclic imine substrate such as benzoxazine, Hopmann found a concerted hydrogenation mechanism implying a single concerted transition state involving simultaneous proton and hydride transfer to the imine (Scheme 39, bottom, **34e**) [115]. This was followed by an amine-mediated hydrogen splitting and proton transfer (**34a**, **34b**, **34c**, **34f**) to regenerate the active

catalyst complex (**34d**) and release the amine product. It is worth to note concerted mechanisms have also been proposed for some bifunctional iridium and ruthenium systems [116-118].

In the presence of a chiral phosphoric acid and a Knölker's complex, the mechanism of imine hydrogenation changed (Scheme 40). Indeed, according to calculations and in agreement with experimental data, the resting state of the catalytic system was in that case the adduct (**35d**) between the iron complex and the deprotonated acid [115].

A hydrogen molecule was coordinated to the iron center and splitted through the cooperation with the phosphoric acid (**31**) to lead to iron hydride species (**35a**), this step being rate limiting. Afterwards, a stepwise mechanism allowed the hydrogenation without any change of oxidation state of the iron(II) Knölker complex. The phosphoric acid interacted with the imine substrate and acted as a proton donor to lead to a transient iminium (**35b**). The latter underwent a hydride transfer under the stereocontrol of the Brønsted acid through non-covalent electrostatic and dispersion interactions between the acid, the substrate and the iron(II) Knölker complex. The resulting amine coordinated to the iron through its nitrogen, the phosphoric acid interacting with the amine and the OH ligand of the iron complex (**35c**). The final release of the amine allowed the resting state of the catalyst (**35d**), the phosphoric acid coordinating to the iron center through its anionic oxygen atom, the other oxygen being H-bonded with the OH ligand of the iron complex. It was worth to note this complete reaction mechanism drew an analogy with the cooperative iridium-catalysed imine AH [119].

Scheme 40. Mechanism of the AH of imines catalysed by a combination of an iron(II) cyclopentadienone dicarbonyl hydride complex **35a** and (*S*)-TRIP Brønsted acid **31** by Hopmann et al.

4.1.2. Iron catalysts based on chelate and macrocyclic ligands.

Following their previous studies, Morris et al. reported the synthesis of several iron(II) complexes based on PNP pincer ligands (Scheme 41) [52,120-122]. *Trans* complexes (**36a**) appeared to afford an interesting pre-catalyst (**36b**) for AH once activated through the imine reduction with LiAlH$_4$ and further reaction with *t*-amyl alcohol. Indeed, the resulting mixture of monohydrides (**36b**) was subsequently applied to the AH of a range of ketones and one imine. Such catalyst proved to be highly active with TOF up to 2000 h^{-1}, TON up to 5000, high conversions and enantioselectivities (up to 85% ee). In spite several NMR experiments and calculations, authors could not clearly establish how many of the possible diastereomeric hydrides led to active catalysts.

Two subsequent studies confirmed such *trans* bromo- or chloro-iron(II) complexes (**37**) and (**38**) based on chiral PNP pincer ligands and comprising or not an imine function were the most active and selective catalysts (up to 96% ee) (Scheme 42).
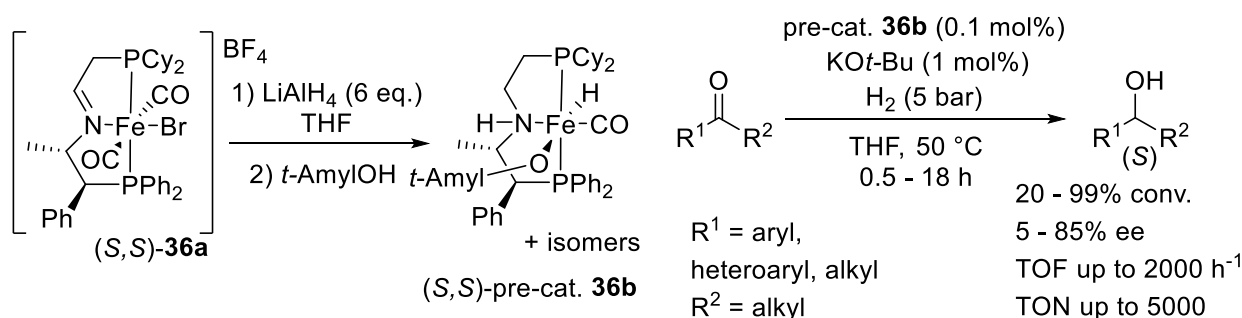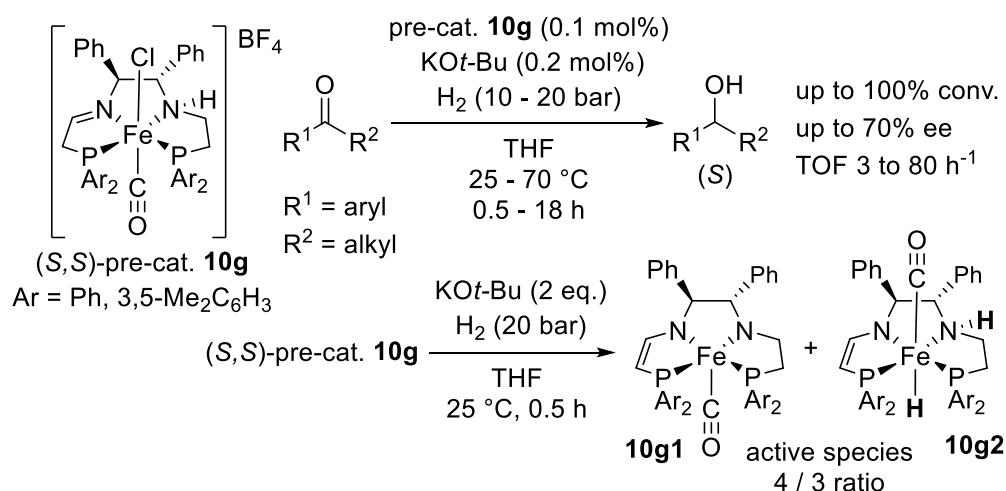
Scheme 41. AH of ketones catalysed by iron(II) hydride complex **36b** based on a chiral PNP ligand by Morris et al.
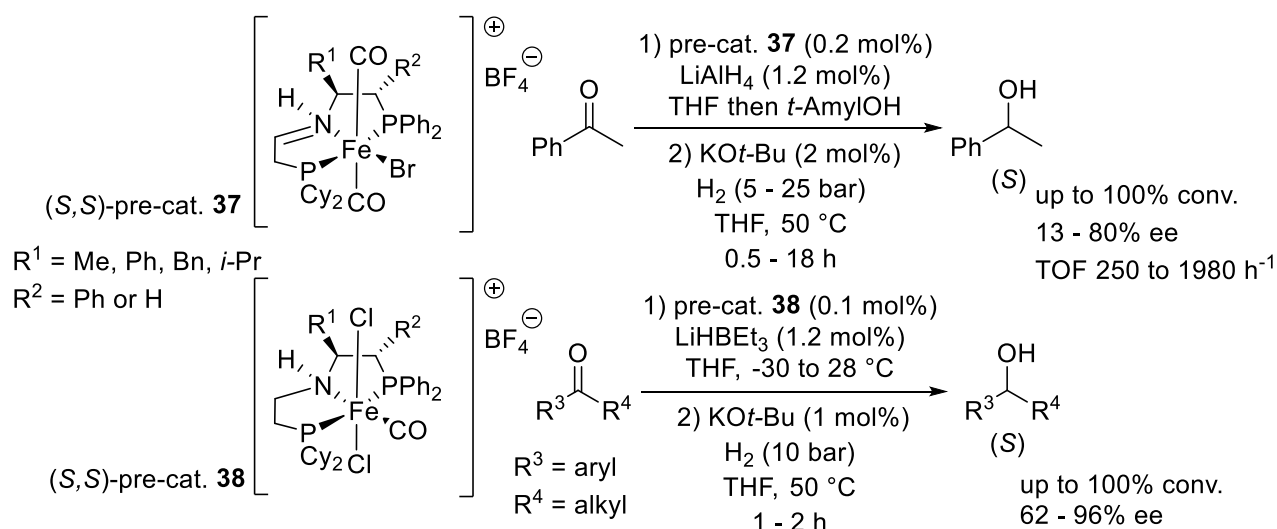
Scheme 42. AH of ketones catalysed by iron(II) halide complexes **37** and **38** based on chiral PNHP ligands by Morris et al.

In 2014, Morris et al. reported also the synthesis of iron(II) complexes (**10g**) with tetradentate amine(imine)diphosphine ligands and their subsequent catalytic applications (Scheme 43) [78]. Activation by a base and hydrogen led to the active amido(ene-amido) (**10g1**) and amine(ene-amido)hydrido (**10g2**) complexes which catalysed the AH of ketones with low to average activities (up to 80 h^{-1} TOF) and enantioselectivities (up to 70% ee). Kinetic studies indicated a reaction rate of zero-order on the ketone concentration and of first-order on the H$_2$ pressure and catalyst concentration. These data confirmed the heterolytic splitting of dihydrogen across the polar iron−nitrogen double bond was the turnover-limiting step in AH as predicted by theoretical calculations.

Scheme 43. AH of ketones catalysed by iron(II) complexes (**10g**) based on a chiral PNNHP ligands by Morris et al.

Afterwards, Morris, Kirchner et al. reported the synthesis of a new chiral PNP′ pincer ligand comprising a planar chiral Ferrocene and a chiral aliphatic amine (Scheme 44) [123]. Metallation with FeBr$_2$ led to a tetrahedral complex which could then react with CO and NaBH$_4$ to yield to the corresponding hydride complex (**39**). The latter subsequently catalysed the AH of ketones with average to high conversions (43-96% conv.) and low to good enantioselectivities (20-81% ee), 1-tetralone leading to the lowest values.
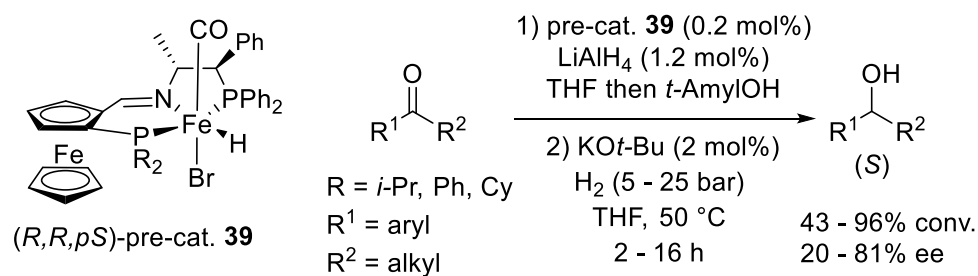
Scheme 44. AH of ketones catalysed by iron(II) complexes based on a chiral PNP Ferrocene ligand by Morris, Kirchner et al.

Through extensive experimental and theoretical studies, Morris et al. adressed several mechanistic issues and proposed a catalytic cycle for their iron(II) catalysed AH of ketones (Scheme 45) [124]. A NMR study confirmed the amine hydride alkoxide complex (**40a**) was the first species in the activation process. Calculations suggested the NH group of the PNHP ligand was then deprotonated by an additional amount of base to form a transient hydride amide complex (**40b**) which could decompose to iron(0) species in the absence of hydrogen gas.

According to NMR experiments, further reaction resulted in the split of dihydrogen via (**40c**) and led to *cis* and *trans* dihydride iron complexes (**40d**). Calculations highlighted the splitting of dihydrogen could proceed with similar energy barriers either at the nitrogen of the hydride amide complex in the inner-coordination sphere, either at the oxygen of the alkoxide group in the outer-coordination sphere. Afterwards, the *trans* dihydride iron complex (**40d**) could react readily with the ketone substrate in the outer coordination sphere similar to ruthenium bifunctional catalysts (Scheme 45, **40e**). The sequential hydride and proton transfer resulted in the alcohol product and released the hydride amide intermediate (**40b**). According to calculations, the hydride transfer and the splitting of dihydrogen had similar energy barriers and could define the rate limiting step and the turn-over frequency depending on the ketone substrate. Finally, the calculated energies of the assumed *pro-S* and *pro-R* transition states were consistent with the observed enantioselectivity
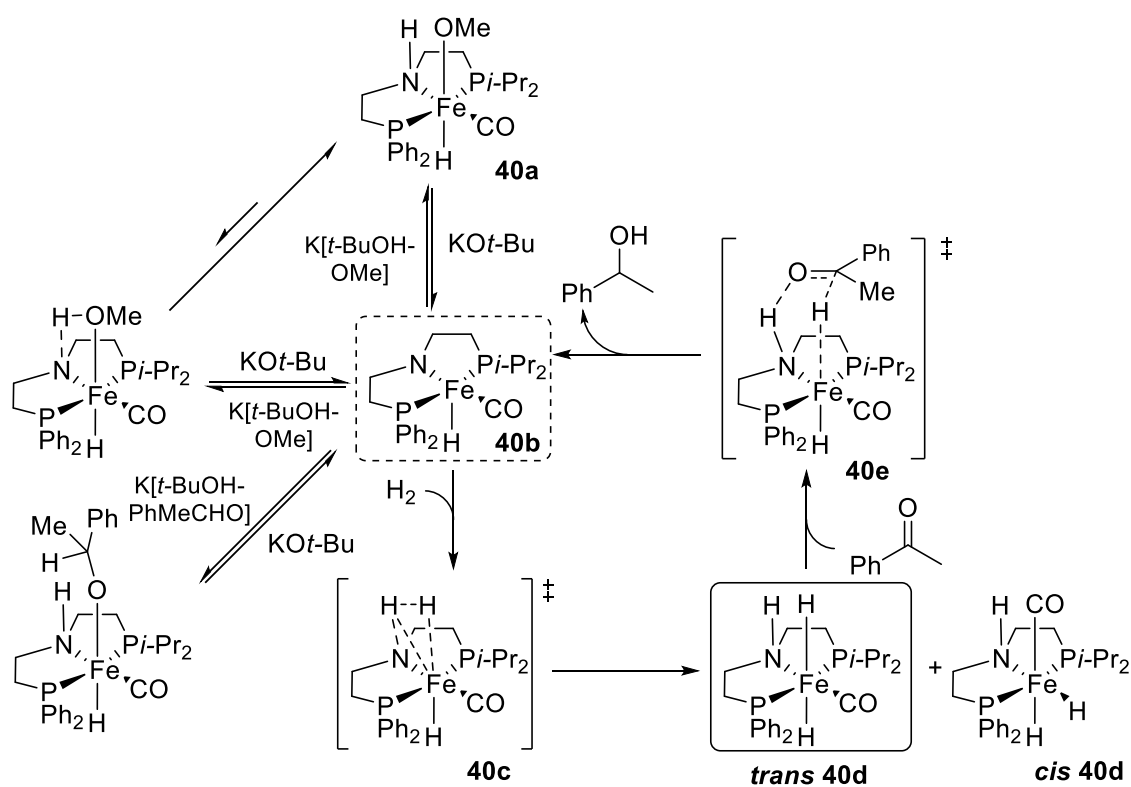
Scheme 45. Mechanism of the AH of ketones catalysed by iron(II) complex **40a** based on a chiral PNHP ligand by Morris et al.

In a recent contribution, Morris et al. reported the application of an unsymmetrical iron PNHP′ pre-catalyst (**41a**) for the AH of imines activated with *N*-diphenylphosphinoyl (Scheme 46) [125]. At the exception of dialkyl derivatives (35% ee), yields (up to 85%) and

enantioselectivities (up to 99% ee) were high. A theoretical study suggested a mechanism starting by the activation of the pre-catalyst (**41a**) through the synthesis of an amine hydride alkoxide complex (**41b**) (Scheme 46). Afterwards, the splitting of dihydrogen proceeded at the oxygen of the alkoxide group with participation of the NH from the hydride complex (**41c**). The resulting *trans* dihydride iron complex (**41d**) reacted with the imine substrate, the PO group of the imine interacting by hydrogen bonding with the N−H group of the iron catalyst. This allowed transition state (**41e**) defined by an eight-membered ring anchoring the *pro-S* face of the imine CN bond over the iron hydride and allowing its transfer which is turnover and enantio-determining.
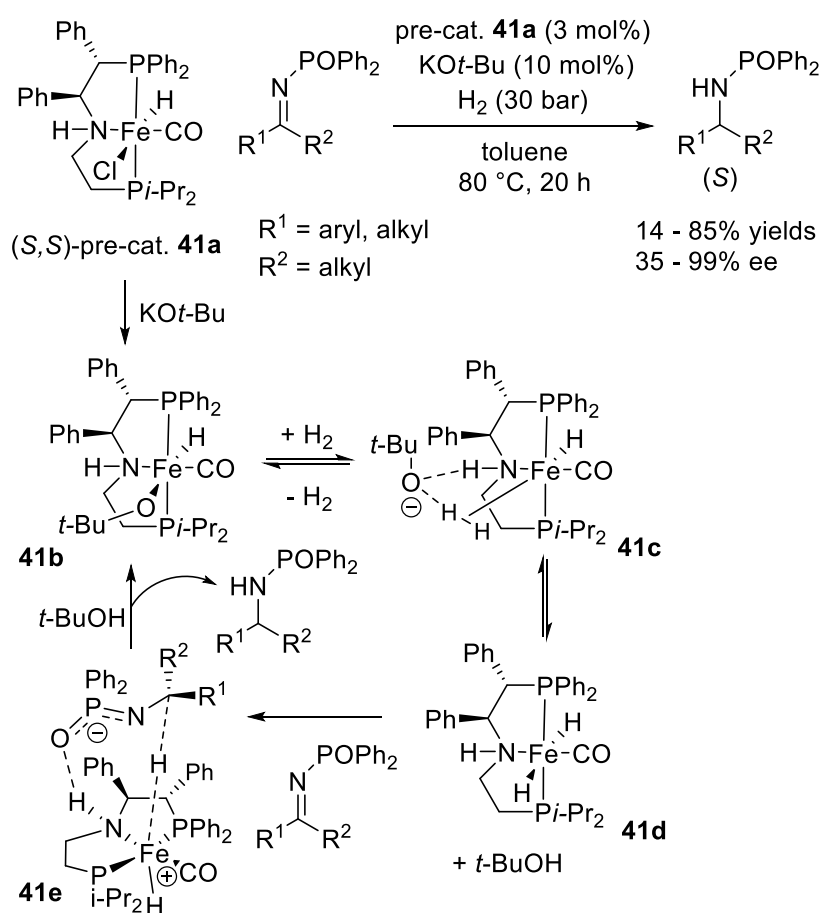
Scheme 46. AH of *N*-diphenylphosphinoyl imines catalysed by iron(II) complex **41a** based on a chiral PNHP ligand by Morris et al.

In parallel, Mezetti et al. reported the synthesis of an iron(II) hydride complex (**42a**) based on a *P*-stereogenic *C₂*-symmetric PNP pincer ligand (Scheme 47) [126]. In the presence of a base, such a complex catalysed the AH of acetophenone to (*S*)-1-phenylethanol in full conversion with 48% ee. The enantiodetermining transfer of hydride to the carbonyl of

acetophenone was studied by theoretical calculations and showed an outer-sphere monohydride mechanism rationalized the experimental asymmetric induction (*S*) and enantioselectivity (Scheme 47), whereas the dihydride and inner-sphere pathways privileged the formation of the (*R*) enantiomer.
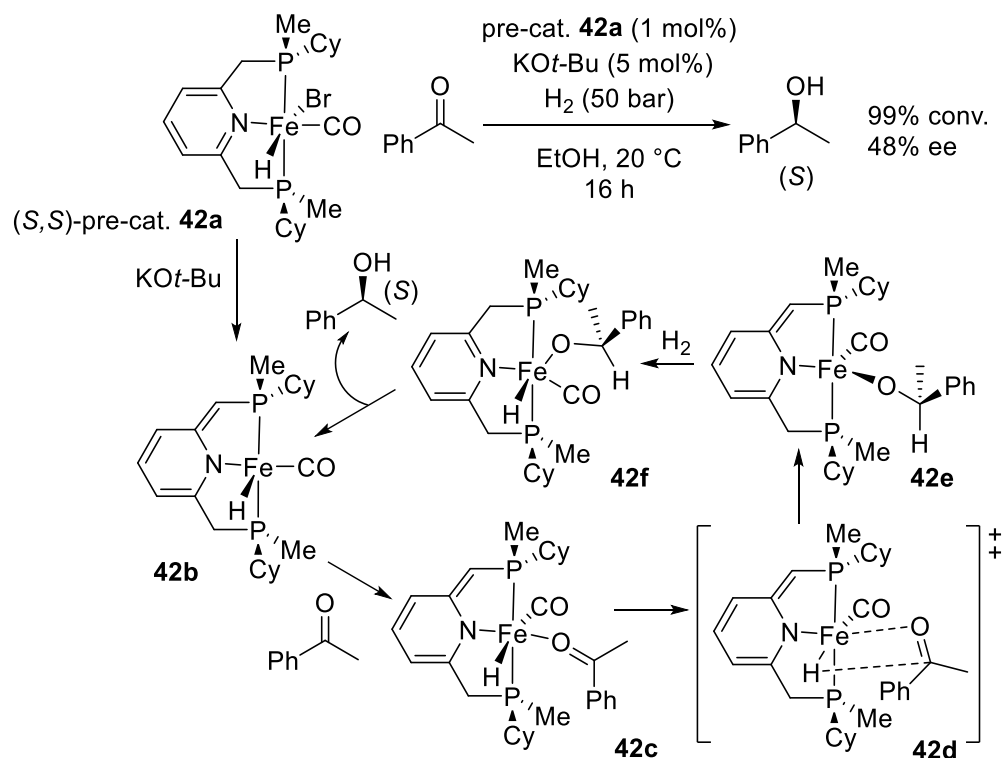
Scheme 47. AH of acetophenone catalysed by an iron(II) complex **42a** based on a chiral PNP ligand by Mezzeti et al.

Mezetti et al. further reported the synthesis of iron(II) hydride complexes (**43**) based on *P*-stereogenic *C$_2$*-symmetric PNHP pincer ligands (Scheme 48) [127]. In the presence of a base, such complexes catalysed the AH of acetophenone to (*S*)-1-phenylethanol in full conversions and with low to average enantioselectivities (19-44% ee).
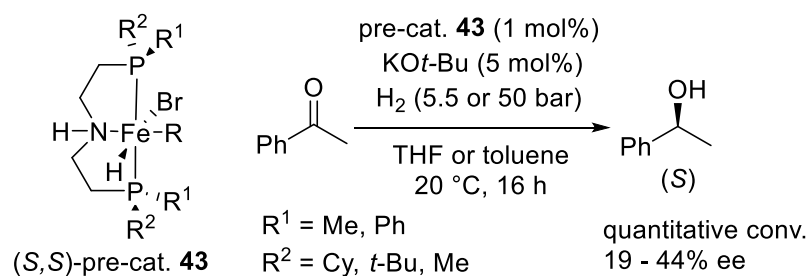
Scheme 48. AH of acetophenone catalysed by iron(II) complexes **43** based on chiral PNHP ligands by Mezzeti et al.

Calculations confirmed the reaction mechanism was similar to the one described by Morris et al. though using different iron(II) catalysts based on *P*-stereogenic PNHP ligands. In addition, authors demonstrated calculations at higher levels of theory helped to take into account non-covalent interactions while designing a ligand by computation.

Afterwards, Beller et al. reported the synthesis of iron(II) borohydride complex (**44**) based on a chiral PNHP pincer ligand with two (2*R*,5*R*)-2,5-dimethyl-phospholane groups (Scheme 49) [128]. Application to the AH of various aromatic and alkyl ketones led to low to high conversions (17-99%) and enantioselectivities (16-99% ee). Theoretical investigations confirmed the reaction mechanism implied a concerted transfer of hydride (from iron) and proton (from the NH) to the ketone substrate. This resulted in the corresponding alcohol product along with an amido iron species which further splitted dihydrogen to allow another reaction.
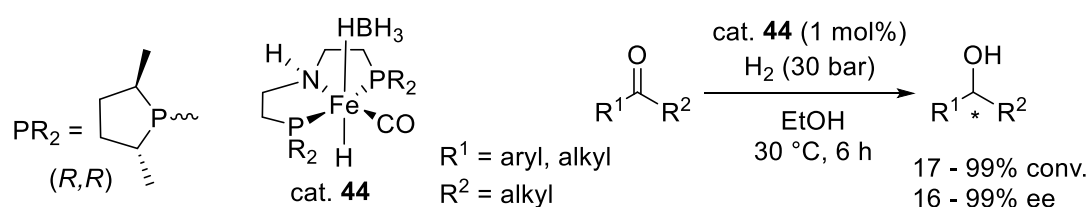
Scheme 49. AH of ketones catalysed by iron(II) complex **44** based on a chiral PNHP ligand by Beller et al.

Starting from 2010, Gao et al. applied iron(0) catalysts based on chiral macrocyclic ligand (**L3**) of $P_2(NH)_4$ type to the AH of various ketones and β-ketoesters (Scheme 50) [60]. Though electron-withdrawing substituents had a negative effect on the course of the substrate hydrogenation, the reduced products were obtained in high yields and enantioselectivities (up to 99% ee for ketones, up to 98% ee for β-ketoesters). Interestingly, authors performed dynamic light scattering (DLS) experiments along their reaction and revealed the presence of nanoparticles. This was also confirmed by poisoning the reaction with additives like PPh_3 or mercury(0). Therefore, by comparison to the molecular iron(II) catalysts developed by the groups of Morris, Mezzeti or Beller, the active catalyst reported by Gao et al. appeared to be iron nanoparticles modified by chiral macrocycles $P_2(NH)_4$.
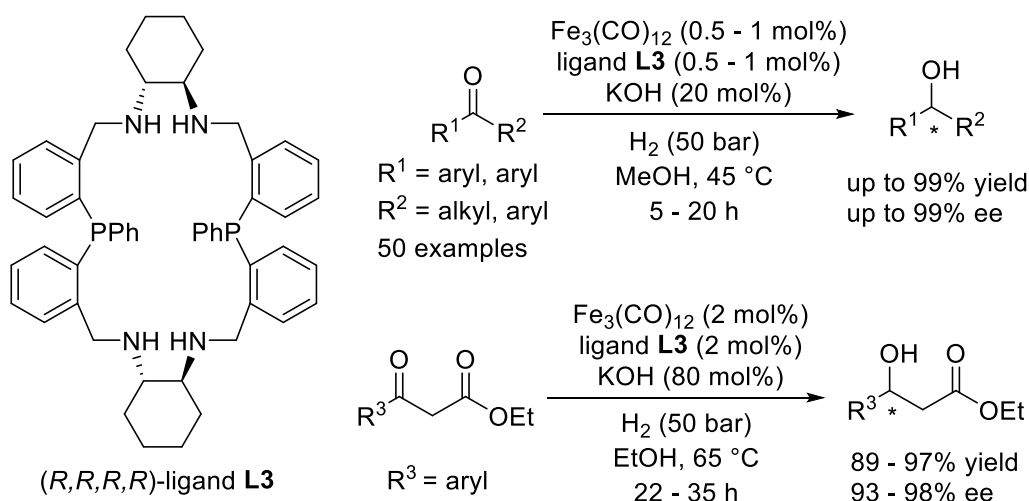
Scheme 50. AH of ketones and β-ketoesters catalysed by a combination of Fe₃(CO)₁₂ and chiral PNHNHPNHNH macrocyclic ligand **L3** by Gao et al.

4.2. Manganese based catalysts.

In 2017, Clarke et al. reported the synthesis of chiral manganese(I) complex (**45**) based on PNN pincer ligand comprising a planar chiral Ferrocene and an amine with point chirality (Scheme 51) [129]. In presence of a catalytic amount of base, the isolated *fac*-manganese complex (**45**) catalysed the AH of various ketones with average to high yields (44-96%) and low to high enantioselectivities (20-91% ee), the catalyst performing better with sterically hindered substrates. The authors assumed a Mn-hydride complex was formed after the loss of one carbonyl and could reduce the ketone substrate similar to iron(II) complexes, the NH group of the ligand being involved in the hydrogen splitting and the enantioselection step.
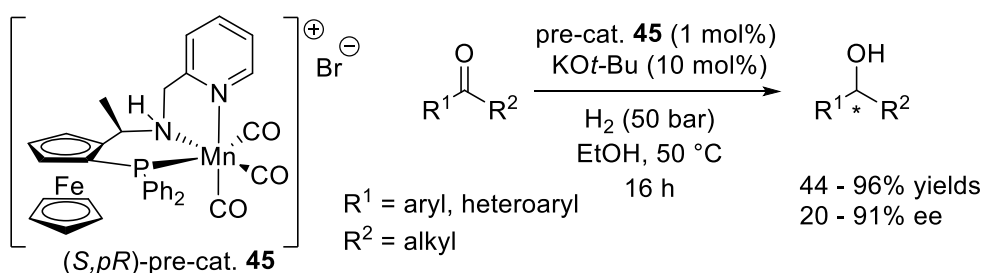
Scheme 51. AH of ketones catalysed by manganese(I) complex **45** based on a chiral PNHN ligand by Clarke et al.

In parallel, Beller et al. reported manganese(I) complex (**46a**) based on a PNP ligand bearing two (2R,5R)-2,5-dimethyl-phospholane groups (Scheme 52) [128,130]. In the presence of a catalytic amount of base, this complex catalysed the AH of a broad scope of ketones in low

to high conversions (26-99%) and low to high enantioselectivities (18-99% ee), aliphatic ketones being more selectively reduced by comparison to Clarke's catalyst. Theoretical calculations suggested the catalysed AH proceeded following an outer-sphere mechanism implying amido (**46b**) and hydride complexes (**46c**) as the key active species. A good agreement was found between calculated and experimental enantioselectivities and absolute configurations.
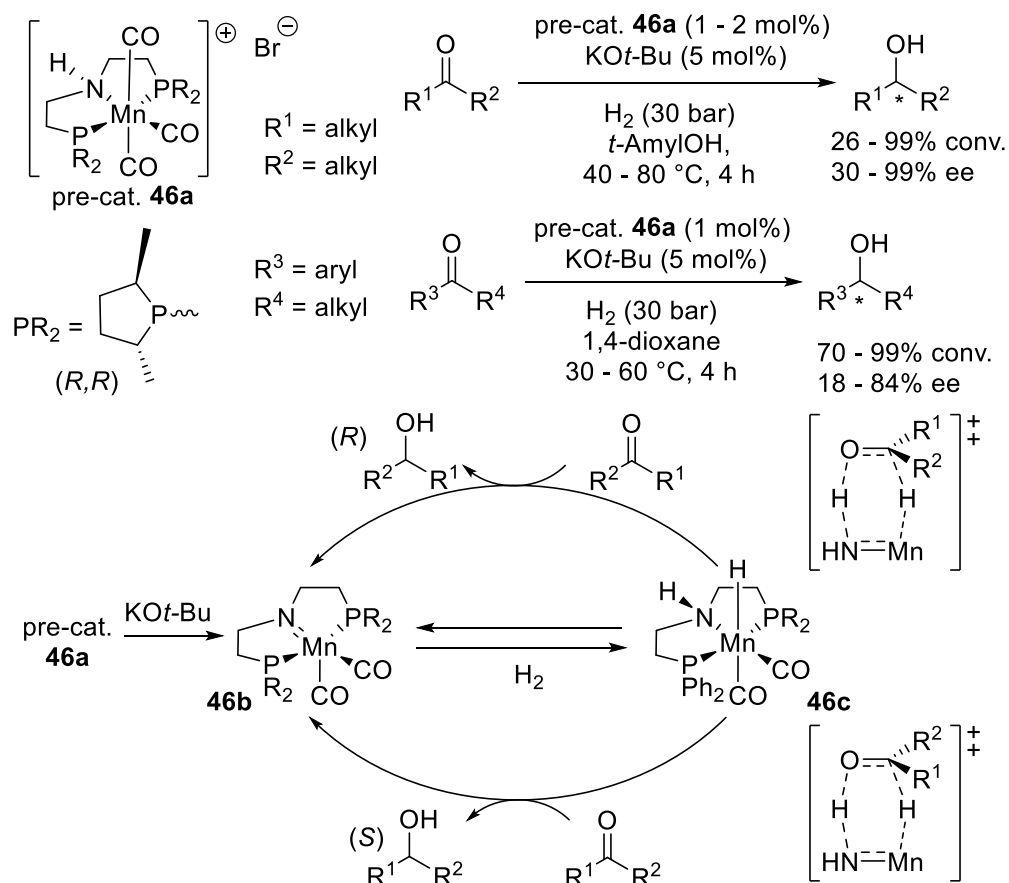
Scheme 52. AH of ketones catalysed by manganese(I) complex **46a** based on a chiral PNHP ligand by Beller et al.

Similarly to Beller et al., Mezzetti et al. reported manganese(I) complex (**47a**) based on a PNHP ligand bearing two chiral phosphine groups (Scheme 53) [131]. The AH of ketones was catalysed in low to high conversions (26-99%) and low to average enantioselectivities (7-55% ee), aliphatic ketones being less selectively reduced by comparison to Beller's catalyst. Afterwards, Mezzetti et al. compared their manganese(I) hydrogenation pre-catalyst (**47a**) with an iron(II) analogue (**48a**) through, experiments, kinetics and theoretical calculations. For both catalysts, the hydrogenation proceeded following an outer-sphere mechanism which implied

amido (**47b**) and hydride (**47d**) complexes (Scheme 53). Moreover, in each case, the hydrogen splitting was the turnover limiting step and the 1-phenylethanolato complex was the off-cycle resting species. The manganese(I) catalyst was found less active than its iron(II) counterpart by a factor of 30 due to a higher stability of the manganese(I) resting species (**47c**) by comparison to the iron(II) ones (**48b**). Indeed, a larger π-delocalization between the alkoxo- and carbonyl ligands was observed for manganese(I) species, the related iron(II) complex having a hydride as *trans* ligand. Finally, the hydrogenation operated through the same bifunctional mechanism with similar transition states around the catalytic cycle and a good agreement was found between calculated and experimental enantioselectivities and the related configurations. In the light of their results, Mezzetti et al. suggested the off-cycle resting manganese(I) alkoxo complex (**47c**) would be less stable and therefore more active while replacing a carbonyl by another ligand.
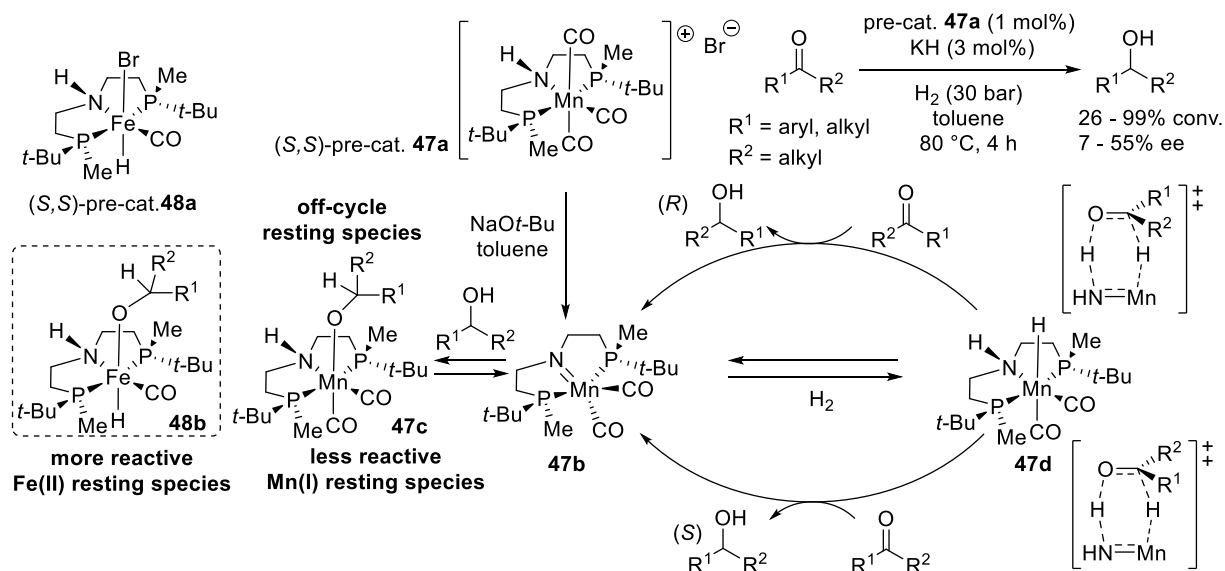
Scheme 53. AH of ketones catalysed by manganese(I) complex **47a** or iron(II) complex **48a** based on a chiral PNHP ligand by Mezzetti et al.

In 2019, Ding et al. reported a highly active manganese(I) hydrogenation catalyst based on a lutidine core with amine and chiral phospholane arms (Scheme 54) [132]. In order to be active, the brominated manganese(I) pre-catalyst (**49**) was combined with catalytic amounts of base and $(CF_3)_2CHOH$ (HFIP), the presence of the latter improving the activities and selectivities. Application to the AH of a wide range of ketones led to high activities with turn-over numbers up to 9800. The resulting alcohols were isolated in nearby quantitative yields and, at the exception of dialkyl derivatives, enantioselectivities were high (up to 97% ee).

Notably, the AH of racemic α-substituted benzofused cyclic ketones led to *cis*-chiral alcohols with high enantioselectivities and diastereoselectivities thanks to an effective dynamic kinetic resolution. According to ³¹P NMR, the pre-catalyst was made of two isomers most likely due to the *syn* and *anti* orientation of the flexible NH fragment as respect to the MnBr bond. Interestingly, a pure *syn* complex with neighbouring *i*-Pr and Br groups was obtained and displayed similar catalytic properties than a mixture of *syn*- and *trans*-isomers. Moreover, the role of the NH fragment in the hydrogen splitting and the enantioselection was confirmed by the poor catalytic results obtained with a *N*-methylated manganese(I) complex. Such observation suggested an outer-sphere hydride mechanism for these catalytic AH.
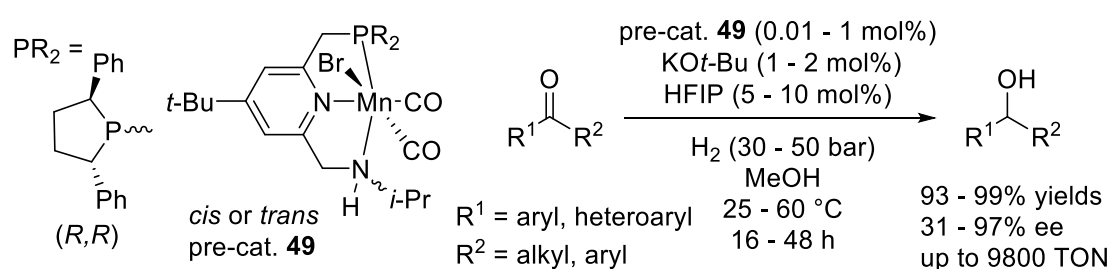
Scheme 54. AH of ketones catalysed by a manganese(I) complex **49** based on a chiral PNP ligand by Ding et al.

In parallel, Zhong et al. prepared manganese(I) complex (**50**) based on PNN ligand (**L9**) comprising a planar chiral Ferrocene, a chiral imine and a tunable benzoimidazole fragment (Scheme 55) [133]. The complex was combined with a base to catalyse AH of *ortho*-halogenated unsymmetrical benzophenones at room temperature and low catalyst loadings. The resulting alcohols were obtained in high yields (up to 99%) and enantiomeric excesses (up to 99% ee) provided the reactions were directed by a halogen substituent, nondirected diaryl ketones leading to poor enantioselectivities. The imine group of the ligand was critical in achieving high activities and enantioselectivities, the related amino ligand leading to partial coordination of the manganese fragment and therefore poor catalytic results. Such a trend confirmed the bifunctional role of the imine group which concomitantly coordinated the metal and activated the hydrogen.
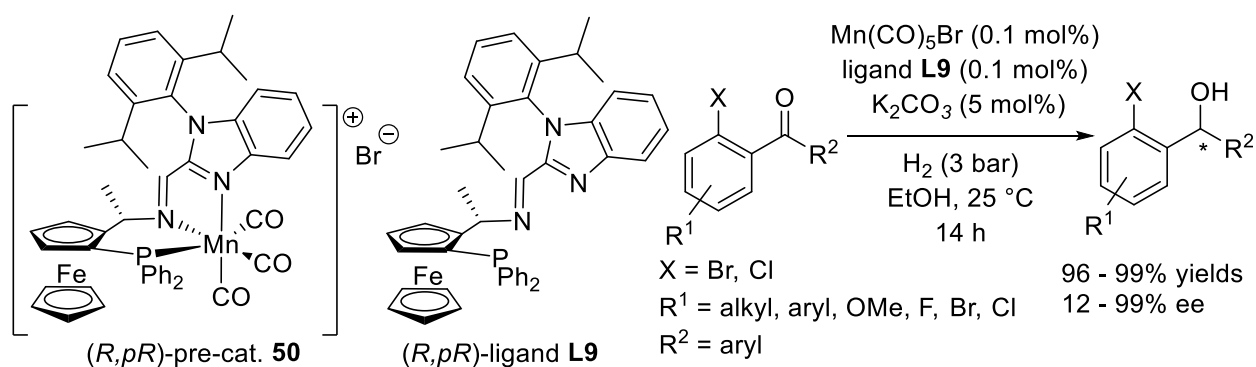
Scheme 55. AH of arylketones catalysed by manganese(I) complex **50** based on a chiral PNP ligand **L9** by Zhong et al.

### 4.3. Cobalt based catalysts.

In a series of publications, Chirik et al. reported the development of chiral C_1-symmetric bis(imino)pyridine cobalt(I) methyl catalyst (**51a**) for the AH of geminal-disubstituted olefins as well as substituted benzofused five-, six-, and seven-membered alkenes (Scheme 56) [134-136]. Yields and enantioselectivities were from average to high and the presence of a coordinating group on the olefin was not required for a stereoselective hydrogenation reaction. Thanks to kinetic studies and various control experiments including isotopic labeling, the authors proposed a catalytic cycle for their hydrogenation reactions [135]. The bis(imino)pyridine cobalt hydride complex (**51b**) formed by reaction of the starting cobalt methyl complex (**51a**) with hydrogen was the catalyst resting state (Scheme 56). The alkene substrate could react either by a fast and reversible 2,1-insertion (**51c**), either by a 1,2-insertion (**51d**) which was the most favorable for the formation of the alkane. Indeed, this turnover-limiting and enantiodetermining step allowed the release of the chiral alkane with a low energy barrier either by cyclohexyl group cyclometalation (**51e**) or by β-hydrogen elimination and further reaction with hydrogen gas. According to additional studies, all cobalt species involved were not redox neutral as depicted in the catalytic cycle and appeared as low-spin cobalt(II), d^7 compounds implied in antiferromagnetic couplings with the ligand bis(imino)pyridine radical anions. Regarding the enantioinduction, the bulkyness of the chiral fragment appeared to control the substrate approach, the alkene interacting with the catalyst from its less sterically hindered side which is its pro-(*S*) face. Finally, such catalyst has recently been applied to the AH of other sterically hindered alkenes [136]. Indeed, a broad scope of 2-alkyl, 2-aryl and 2-boryl-substituted 1,1-diboryl alkenes was hydrogenated in high yields and enantioselectivities.
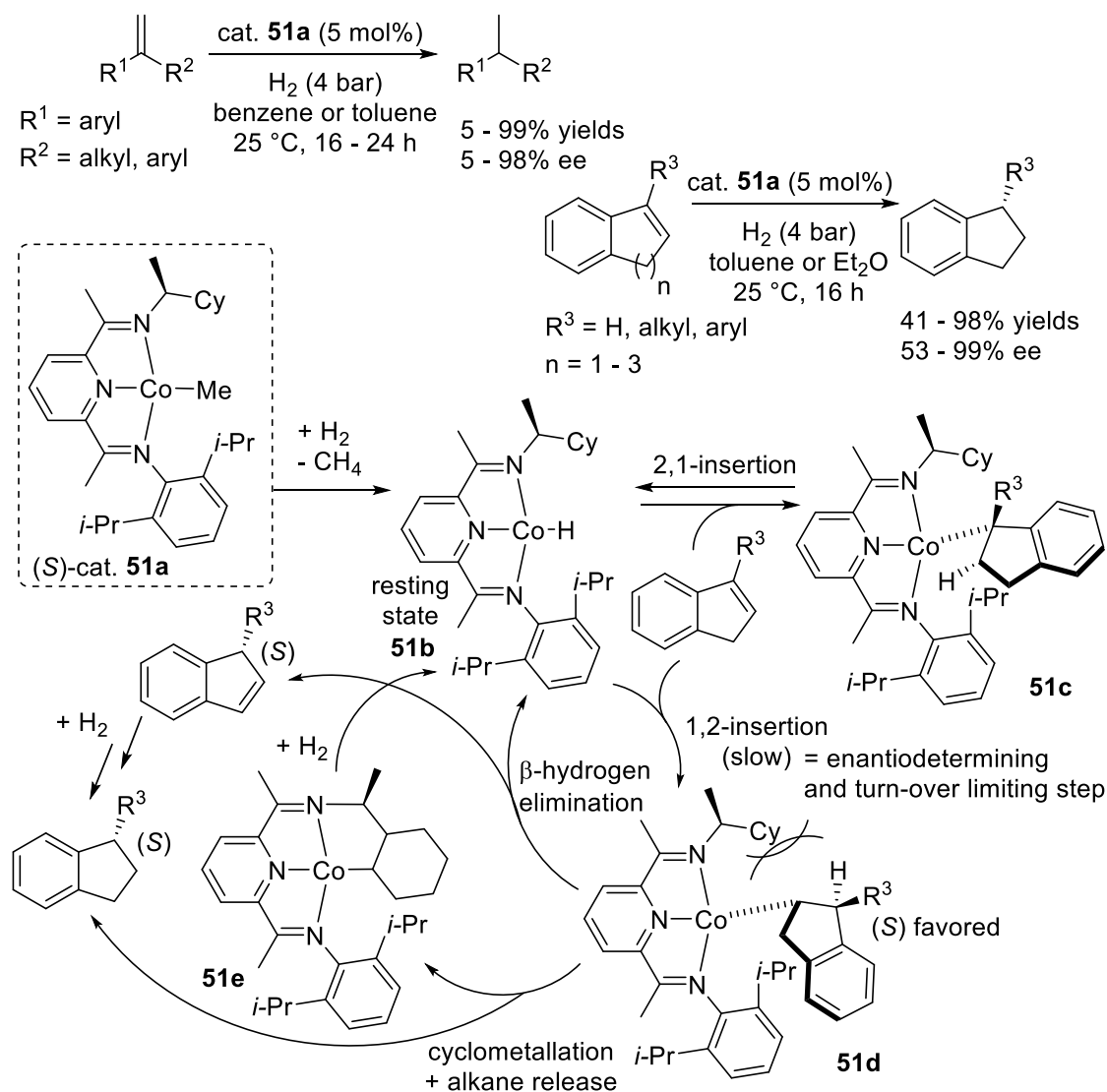
Scheme 56. AH of alkenes catalysed by cobalt(I) complex **51a** based on a chiral NNN ligand by Chirik et al.

In 2016, Gao et al. reported the preparation of cobalt(II) complex (**52**) by refluxing PNHNHP ligand and CoCl$_2$ in acetonitrile under nitrogen (Scheme 57) [137]. While the synthesis was performed under air, authors noticed the formation of complex (**53**) due to the oxidation of one phosphine ligand. Though both paramagnetic complexes catalysed the AH of ketones, they required an important excess of base in methanol (4 equivalents) to be active and rather long reaction times were necessary to reach high yields (48 h). By comparison to its non-oxidized analogue, the pre-catalyst (**53**) bearing a PNHNHPO ligand displayed higher activities (up to 99% yield) and enantioselectivities (up to 95% ee).
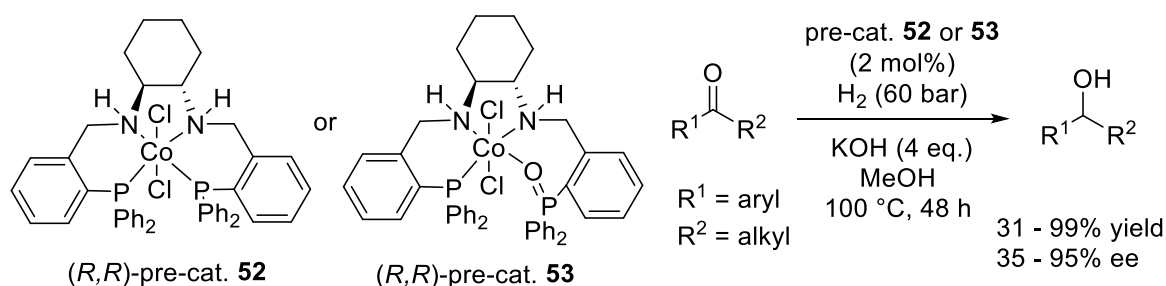
Scheme 57. AH of ketones catalysed by cobalt(II) complexes **52** or **53** based on a chiral PNHNHP ligand by Gao et al.

5. Conclusion

Bifunctional catalysts based on first row transition metals have widely been applied to asymmetric hydrogenations (AH) along the past decade. The rise of earth-abundant metals like iron and manganese, and to a lesser extent cobalt and nickel, has been confirmed through previous catalyst modifications or design of new ligands like pincers or macrocycles. Cooperative approaches have been developed in order to allow specific non-covalent interactions between the catalysts ligand and the substrate for activation and enantioselection benefits. It is worth to note most of these achievements have been accomplished thanks to a deep understanding of the catalysts nature through the combination of synthetic and reactivity developments, structural and kinetic studies as well as theoretical calculations. Interestingly, some of these effective and selective catalysts proved to be no longer homogenous but heterogeneous due to the presence of well-defined paramagnetic chiral nanoparticles [60,84-86].

Nowadays, both asymmetric hydrogenation (AH) and asymmetric transfer hydrogenation (ATH) rely on well-established catalytic systems exhibiting complementary properties in terms of activities and stereo-, chemo- and regioselectivities. Indeed, a great diversity of organic substrates with carbonyl, imine or olefin functions can be hydrogenated with high selectivities [39]. Nevertheless, several challenges remain to be met. Because no general solution can be found for catalytic asymmetric hydrogenation of organic compounds, there's a continuous need of new catalysts [39]. Furthermore, the asymmetric hydrogenation of substrates like alkyl ketones and imines [138], carbocyclic arenes [139,140], some nitrogen based heterocycles [141], tri- and tetrasubstituted alkenes [141,142] is still challenging. In addition, the development of chemoselective catalytic processes, i.e. catalysts tolerating other functional groups, remains highly desirable [143]. Due to economic, environmental and societal

reasons, hydrogenation catalysts based on abundant metals [144,145] have kept chemist's interest over the past decade and we have seen significants achievements have been reported using bifunctional catalysts. From an industrial perspective [146,147], the development of highly active catalysts, i.e. high turnover number catalysts, at low costs and with possible applications in flow chemistry appear as the main goal to fulfil [148-151].

References:

[1] R. Noyori in: Asymmetric Catalysis in Organic Synthesis, chapter 2, Wiley, New York, 1994.

[2] T. Ohkuma, M. Kitamura, R. Noyori in: I. Ojima (Ed.), Catalytic Asymmetric Synthesis 2nd Edition, p 1, Wiley-VCH, 2000.

[3] H.-U. Blaser, H.-J. Federsel in Asymmetric Catalysis on Industrial Scale, Wiley-VCH, 2010.

[4] W. S. Knowles, Angew. Chem. Int. Ed. 41 (2002) 1998−2007.

[5] R. Noyori, Angew. Chem. Int. Ed. 41 (2002) 2008−2022.

[6] R. Noyori, Adv. Synth. Catal. 345 (2003) 15−32.

[7] H. U. Blaser, B. Pugin, F. Spindler, L. A. Saudan in: B. Cornils, W. A Herrmann, M. Beller, R. Paciello (Ed.), Applied Homogeneous Catalysis with Organometallic Compounds 3rd Edition, p 621−690, Wiley-VCH, 2018.

[8] F. Foubelo, C. Najera, M. Yus. Tetrahedron: Asym. 26 (2015) 769−790.

[9] H. G. Nedden, A. Zanotti-Gerosa, M. Wills, Chem. Record *16* (2016) 2619−2639.

[10] B. Stefane, F. Pozgan, Topics in Current Chem. 374 (2016) 1−67.

[11] D. Wang, D. Astruc, Chem. Rev. 115 (2015) 6621−6686.

[12] A. Matsunami, Y. Kayaki, Tetrahedron Lett. 59 (2018) 504−513.

[13] E. Baráth, Catalysts 8 (2018) 671−696.

[14] P. Etayo, A. Vidal-Ferran, Chem. Soc. Rev. 42 (2013), 728−754.

[15] T. Ohkuma, R. Noyori, Angew. Chem. Int. Ed. 40 (2001) 40−73.

[16] T. Ohkuma, H. Ooka, S. Hashiguchi, T. Ikariya, R. Noyori, J. Am. Chem. Soc. 117 (1995) 2675–2676.

[17] S. Hashiguchi, A. Fujii, J. Takehara, T. Ikariya, R. Noyori, J. Am. Chem. Soc. 117 (1995) 7562–7563.

[18] R. Noyori, T. Ohkuma, Pure Appl. Chem. 71 (1999) 1493–1501.

[19] T. Ohkuma, M. Koizumi, K. Muñiz, G. Hilt, C. Kabuto, R. Noyori, J. Am. Chem. Soc. 124 (2002) 6508–6509.

[20] R. Noyori, S. Hashiguchi, Acc. Chem. Res. 30 (1997) 97−102.

[21] M. J. Palmer, M. Wills, Tetrahedron Asym. 10 (1999) 2045−2061.

[22] S. Clamham, A. Hadzovic, R. H. Morris, Coord. Chem. Rev. 248 (2004) 2201–2237.

[23] K.-J. Haack, S. Hashiguchi, A. Fujii, T. Ikariya, R. Noyori, Angew. Chem. Int. Ed. 36 (1997) 285−288.

[24] C. P. Casey, J. B. Johnson, J. Org. Chem. 68 (2003) 1998–2001.

[25] C. A. Sandoval, T. Ohkuma, K. Muñiz, R. Noyori, J. Am. Chem. Soc. 125 (2003) 13490–13503.

[26] D. A. Alonso, P. Brandt, S. J. M. Nordin, P. G. Andersson, J. Am. Chem. Soc. 121 (1999) 9580–9588.

[27] M. Yamakawa, H. Ito, R. Noyori, J. Am. Chem. Soc. 122 (2000) 1466–1478.

[28] S. M. Joseph, J. S. Samec, J.-E. Bäckvall, P. G. Andersson, P. Brandt, Chem. Soc. Rev. 35 (2006) 237–248.

[29] T. Ikariya, K. Murata, R. Noyori, Org. Biomol. Chem. 4 (2006) 393−406.

[30] T. Ikariya, A. J. Blacker, Acc. Chem. Res. 40 (2007) 1300−1308.

[31] M. Sawamura, Y. Ito, Chem. Rev. 92 (1992) 857–871.

[32] H. Steinhagen, G. Helmchen, Angew. Chem. Int. Ed. 35 (1996) 2339–2342.

[33] M. Shibasaki, H. Sasai, T. Arai, Angew. Chem. Int. Ed. 36 (1997) 1236–1256.

[34] E. K. Van den Beuken, B. L. Feringa, Tetrahedron 54 (1998) 12985–13011.

[35] G. J. Rowlands, Tetrahedron 57 (2001) 1865–1882.

[36] H. Gröger, Chem. Eur. J. 7 (2001) 5246–5251.

[37] M. Shibasaki, N. Yoshikawa, Chem. Rev. 102 (2002) 2187–2209.

[38] J.-A. Ma, D. Cahard, Angew. Chem. Int. Ed. 43 (2004) 4566–4583.

[39] C. S. G. Seo, R. H. Morris, Organometallics 38 (2019) 47−65.

[40] T. Ikariya, Y. Kayaki, Pure Applied Chem. 86 (2014) 933−943.

[41] X.-Q. Dong, Q. Zhao, P. Li, C. Chen, X. Zhang, Org. Chem. Front. 2 (2015) 1425−1431.

[42] I. D. Gridnev, ChemCatChem 8 (2016) 3463−3465.

[43] J. Zhang, J. Jia, X. Zeng, Y. Wang, Z. Zhang, I. D. Gridnev, W. Zhang, Angew. Chem. Int. Ed. 58 (2019) 11505−11512.

[44] J. Chen, I. D. Gridnev, iScience 23 (2020) 100960−100972.

[45] A. Correa, O. G. Mancheno, C. Bolm, Chem. Soc. Rev. 37 (2008) 1108–1117.

[46] C. Wang, X. F. Wu, J. L. Xiao, Chem. Asian J. 3 (2008) 1750–1770.

[47] P. J. Chirik in: R. M. Bullock (Ed), Catalysis without Precious Metals; p 83–110, Wiley-VCH, 2010.

[48] M. S. Holzwarth, B. Plietker, ChemCatChem 5 (2013) 1650–1679.

[49] S. W. M. Crossley, C. Obradors, R. M. Martinez, R. A. Shenvi, Chem. Rev. 116 (2016) 8912–9000.

[50] F. Kallmeier, R. Kempe, Angew. Chem. Int. Ed. 57 (2018) 46–60.

[51] R. H. Morris, Chem. Soc. Rev. 38 (2009) 2282–2291.

[52] R. H. Morris, Acc. Chem. Res. 48 (2015) 1494−1502.

[53] R. H. Morris, Chem. Record 16 (2016) 2640−2654.

[54] P. E. Sues, K. Z. Demmans, R. H. Morris, Dalton Trans. 43 (2014) 7650−7667.

[55] S. Kuwata, T. Ikariya, Dalton Trans. 39 (2010), 2984−2992.

[56] D. B. Grotjahn, Pure Applied Chem. 82 (2010) 635−647.

[57] C. T. Mbofana, S. J. Miller in: E. Vedejs, S. E. Denmark (Ed.), From Lewis Base Catalysis in Organic Synthesis; p 1259−1288, Wiley-VCH, 2016.

[58] R. ter Halle, A. Bréhéret, E. Schulz, C. Pinel, M. Lemaire, Tetrahedron Asym. 8 (1997) 2101−2108.

[59] J. S. Chen, L. L. Chen, Y. Xing, G. Chen, W. Y. Shen, Z. R. Dong, Y. Y. Li, J. X. Gao, Acta Chim. Sinica 62 (2004) 1745−1750.

[60] Y.-Y. Li, S.-L. Yu, W.-Y. Shen, J.-X. Gao, Acc. Chem. Res. 48 (2015) 2587−2598.

[61] C. Sui-Seng, F. Freutel, A. J. Lough, R. H. Morris, Angew. Chem. Int. Ed. 47 (2008) 940−943.

[62] C. Sui-Seng, F. N. Haque, A. Hadzovic, A.-M. Pütz, V. Reuss, N. Meyer, A. J. Lough, M. Z.-D. Iuliis, R. H. Morris, Inorg. Chem. 48 (2009) 735−743.

[63] A. A. Mikhailine, E. Kim, C. Dingels, A. J. Lough, R. H. Morris, Inorg. Chem. 47 (2008) 6587−6589.

[64] A. A. Mikhailine, A. J. Lough, R. H. Morris, J. Am. Chem. Soc. 131 (2009) 1394−1395.

[65] I. Bauer, H.-J. Knölker, Chem. Rev. 115 (2015) 3170–3387.

[66] J. P. Hopewell, J. E. D. Martins, T. C. Johnson, J. Godfrey, M. Wills, Org. Biomol. Chem. 10 (2012), 134−145.

[67] R. Hodgkinson, A. Del Grosso, G. Clarkson, M. Wills, Dalton Trans. 45 (2016) 3992–4005.

[68] C. A. M. R. van Slagmaat, K. C. Chou, L. Morick, D. Hadavi, B. Blom, S. M. A. De Wildeman, Catalysts 9 (2019) 790−814.

[69] S. Zhou, S. Fleischer, K. Junge, S. Das, D. Addis, M. Beller, Angew. Chem. Int. Ed. 49 (2010) 8121−8125.

[70] P. O. Lagaditis, A. J. Lough, R. H. Morris, Inorg. Chem. 49 (2010) 10057−10066.

[71] A. A. Mikhailine, R. H. Morris, Inorg. Chem. 49 (2010) 11039−11044.

[72] P. E. Sues, A. J. Lough, R. H. Morris, Organometallics 30 (2011) 4418−4431.

[73] A. A. Mikhailine, M. I. Maishan, R. H. Morris, Org. Lett. 14 (2012) 4638−4641.

[74] A. A. Mikhailine, M. I. Maishan, A. J. Lough, R. H. Morris, J. Am. Chem. Soc. 134 (2012), 12266−12280.

[75] P. O. Lagaditis, A. J. Lough, R. H. Morris, J. Am. Chem. Soc. 133 (2011) 9662−9665.

[76] W. Zuo, D. E. Prokopchuk, A. J. Lough, R. H. Morris, ACS Catal. 6 (2016) 301−314.

[77] W. Zuo, A. J. Lough, Y. F. Li, R. H. Morris, Science 342 (2013) 1080−1083.

[78] W. Zuo, S. Tauer, D. E. Prokopchuk, R. H. Morris, Organometallics 33 (2014) 5791−5801.

[79] W. Zuo, R. H. Morris, Nature Protocols 10 (2015) 241−257.

[80] S. A. M. Smith, R. H. Morris, Synthesis 47 (2015) 1775−1779.

[81] S. A. M. Smith, D. E. Prokopchuk, R. H. Morris, Israel J. Chem. 57 (2017) 1204−1215.

[82] K. Z. Demmans, O. W. K. Ko, R. H. Morris, RSC Adv. 6 (2016), 88580−88587.

[83] K. Z. Demmans, C. S. G. Seo, A. J. Lough, R. H. Morris, Chem. Sci. 8 (2017) 6531−6541.

[84] J. F. Sonnenberg, N. Coombs, P. A. Dube, R. H. Morris, J. Am. Chem. Soc. 134 (2012) 5893−5899.

[85] J. F. Sonnenberg, R. H. Morris, Catal. Sci. Technol. 4 (2014) 3426−3438.

[86] P. O. Lagaditis, P. E. Sues, A. J. Lough, R. H. Morris, Dalton Trans. 44 (2015) 12119−12127.

[87] R. Bigler, A. Mezzetti, Org. Lett. 16 (2014) 6460−6463.

[88] R. Bigler, E. Otth, A. Mezzetti, Organometallics 33 (2014) 4086−4099.

[89] R. Bigler, R. Huber, A. Mezzetti, Angew. Chem. Int. Ed. 54 (2015) 5171−5174.

[90] R. Bigler, A. Mezzetti, Org. Proc. Res. Dev. 20 (2016) 253−261.

[91] R. Bigler, R. Huber, M. Stockli, A. Mezzetti, ACS Catal. 6 (2016) 6455−6464.

[92] L. De Luca, A. Mezzetti, Angew. Chem. Int. Ed. 56 (2017) 11949−11953.

[93] L. De Luca, A. Passera, A. Mezzetti, J. Am. Chem. Soc. 141 (2019) 2545−2556.

[94] S. L. Yu, W. Y. Shen, Y. Y. Li, Z. R. Dong, Y. Q. Xu, Q. Li, J. N. Zhang, J. X. Gao, Adv. Synth. Catal. 354 (2012) 818−822.

[95] A. Zirakzadeh, S. R. M. M. de Aguiar, B. Stöger, M. Widhalm, K. Kirchner, ChemCatChem 9 (2017) 1744−1748.

[96] D. Wang, A. Bruneau-Voisine, J.-B. Sortais, Catal. Commun. 105 (2018) 31−36.

[97] K. Azouzi, A. Bruneau-Voisine, L. Vendier, J.-B. Sortais, S. Bastin, Catal. Commun. 142 (2020) 106040−106045.

[98] K. Z. Demmans, M. E. Olson, R. H. Morris, Organometallics 37 (2018) 4608−4618.

[99] J. Schneekoenig, K. Junge, M. Beller, Synlett 30 (2019) 503−507.

[100] R. van Putten, G. A. Filonenko, A. G. de Castro, C. Liu, M. Weber, C. Müller, L. Lefort, E. Pidko, Organometallics 38 (2019) 3187−3196

[101] A. Passera, A. Mezzetti, Angew. Chem. Int. Ed. 59 (2020) 187−191.

[102] Z. R. Dong, Y. Y. Li, S. L. Yu, G. S. Sun, J. X. Gao, Chin. Chem. Lett. 23 (2012) 533−536.

[103] A. Berkessel, S. Reichau, A. von der Höh, N. Leconte, J.-M. Neudörfl, Organometallics 30 (2011) 3880–3887.

[104] P. Gajewski, M. Renom-Carrasco, S. Vailati Facchini, L. Pignataro, L. Lefort, J. G. de Vries, R. Ferraccioli, A. Forni, U. Piarulli, C. Gennari, Eur. J. Org. Chem. 2015 (2015) 1887–1893.

[105] P. Gajewski, M. Renom-Carrasco, S. Vailati Facchini, L. Pignataro, L. Lefort, J. G. de Vries, R. Ferraccioli, U. Piarulli, C. Gennari, Eur. J. Org. Chem. 2015 (2015) 5526−5536.

[106] M. Cettolin, X. Bai, D. Lübken, M. Gatti, S. Vailati Facchini, U. Piarulli, L. Pignataro, C. Gennari, Eur. J. Org. Chem. 2019 (2019) 647−654.

[107] D. S. Mérel, S. Gaillard, T. R. Ward, J.-L. Renaud, Catal. Lett. 146 (2016), 564–569.

[108] D. Brenna, S. Rossi, F. Cozzi, M. Benaglia, Org. Biomol. Chem. 15 (2017) 5685−5688.

[109] A. Del Grosso, A. E. Chamberlain, G. J. Clarkson, M. Wills, Dalton Trans. 47 (2018) 1451–1470.

[110] X. Bai, M. Cettolin, G. Mazzoccanti, M. Pierini, U. Piarulli, V. Colombo, A. Dal Corso, L. Pignataro, C. Gennari, Tetrahedron 75 (2019) 1415−1424.

[111] S. Zhou, S. Fleischer, K. Junge, M. Beller, Angew. Chem. Int. Ed. 50 (2011), 5120–5124.

[112] S. Fleischer, S. Zhou, S. Werkmeister, K. Junge, M. Beller, Chem. Eur. J 19 (2013), 4997−5003.

[113] S. Fleischer, S. Werkmeister, S. Zhou, K. Junge, M. Beller, Chem. Eur. J. 18 (2012), 9005−9010.

[114] A. von der Höh, A. Berkessel, ChemCatChem 3 (2011), 861−867.

[115] K. Hopmann, Chem. Eur. J. 21 (2015) 10020−10030.

[116] M. Martín, E. Sola, S. Tejero, J. L. Andres, L. A. Oro. Chem. Eur. J. 12 (2006) 4043−4056.

[117] A. Comas-Vives, G. Ujaque, A. Lledós. Organometallics 27 (2008) 4854−4863.

[118] T. Nagano, A. Iimuro, R. Schwenk, T. Ohshima, Y. Kita, A. Togni, K. Mashima. Chem. Eur. J. 18 (2012) 11578−11592.

[119] W. Tang, S. Johnston, J. A. Iggo, N. G. Berry, M. Phelan, L. Lian, J. Bacsa, J. Xiao, Angew. Chem. Int. Ed. 52 (2013) 1668−1672.

[120] P. O. Lagaditis, P. E. Sues, J. F. Sonnenberg, K. Y. Wan, A. J. Lough, R. H. Morris, J. Am. Chem. Soc. 136 (2014) 1367−1380.

[121] J. F. Sonnenberg, A. J. Lough, R. H. Morris, Organometallics 33 (2014) 6452−6465.

[122] S. A. M. Smith, P. O. Lagaditis, A. Luepke, A. J. Lough, R. H. Morris, Chem. Eur. J. 23 (2017) 7212−7216.

[123] A. Zirakzadeh, K. Kirchner, A. Roller, B. Stöger, M. Widhalm, R. H. Morris, Organometallics 35 (2016) 3781−3787.

[124] J. F. Sonnenberg, K. Y. Wan, P. E. Sues, R. H. Morris, ACS Catalysis 7 (2017) 316−326.

[125] C. S. G. Seo, T. Tannoux, S. A. M. Smith, A. J. Lough, R. H. Morris, J. Org. Chem. 84 (2019) 12040−12049.

[126] R. Huber, A. Passera, A. Mezzetti, Organometallics 37 (2018) 396−405.

[127] R. Huber, A. Passera, E. Gubler, A. Mezzetti, Adv. Synth. Catal. 360 (2018) 2900−2913.

[128] M. Garbe, Z. Wei, B. Tannert, A. Spannenberg, H. Jiao, S. Bachmann, M. Scalone, K. Junge, M. Beller, Adv. Synth. Catal. 361 (2019) 1913−1920.

[129] M. B. Widegren, G. J. Harkness, A. M. Z. Slawin, D. B. Cordes, M. L. Clarke, Angew. Chem. Int. Ed. 56 (2017) 5825–5828.

[130] M. Garbe, K. Junge, S. Walker, Z. Wei, H. Jiao, A. Spannenberg, S. Bachmann, M. Scalone, M. Beller, Angew. Chem. Int. Ed. 56 (2017) 11237−11241.

[131] A. Passera, A. Mezzetti, Adv. Synth. Catal. 361 (2019) 4691−4706.

[132] L. Zhang, Y. Tang, Z. Han, K. Ding, Angew. Chem. Int. Ed. 58 (2019) 4973−4977.

[133] F. Ling, H. Hou, J. Chen, S. Nian, X. Yi, Z. Wang, D. Song, W. Zhong, Org. Lett. 21 (2019) 3937−3941.

[134] S. Monfette, Z. R. Turner, S. P. Semproni, P. J. Chirik, J. Am. Chem. Soc. 134 (2012) 4561−4564.

[135] M. R. Friedfeld, M. Shevlin, G. W. Margulieux, L. C. Campeau, P. J. Chirik, J. Am. Chem. Soc. 138 (2016) 3314−3324.

[136] P. Viereck, S. Krautwald, T. P. Pabst, P. J. Chirik, J. Am. Chem. Soc. 142 (2020) 3923−3930.

[137] D. Zhang, E.-Z. Zhu, Z.-W. Lin, Z.-B. Wei, Y.-Y. Li, J.-X. Gao, Asian J. Org. Chem. 5 (2016) 1323−1326.

[138] T. Ohkuma, C. A. Sandoval, R. Srinivasan, Q. Lin, Y. Wei, K. Muniz, R. Noyori, J. Am. Chem. Soc. 127 (2005) 8288−8289.

[139] R. Kuwano, R. Morioka, M. Kashiwabara, N. Kameyama, Angew. Chem. Int. Ed. 51 (2012) 4136−4139.

[140] D.-S. Wang, Q.-A. Chen, S.-M. Lu, Y.-G. Zhou, Chem. Rev. 112 (2012) 2557−2590.

[141] C. Margarita, P. G. Andersson, J. Am. Chem. Soc. 139 (2017) 1346−1356.

[142] S. Kraft, K. Ryan, R. B. Kargbo, J. Am. Chem. Soc. 139 (2017) 11630−11641.

[143] T. Gensch, M. Teders, F. Glorius, J. Org. Chem. 82 (2017) 9154−9159.

[144] R. M. Bullock, Science 342 (2013) 1054−1055.

[145] J. R. Ludwig, C. S. Schindler, Chem 2 (2017) 313−316.

[146] J. A. Gladysz, Pure Appl. Chem. 73 (2001) 1319−1324.

[147] S. Hübner, J. G. de Vries, V. Farina, Adv. Synth. Catal. 358 (2016) 3−25.

[148] R. Duque, P. J. Pogorzelec, D. J. Cole-Hamilton, Angew. Chem. Int. Ed. 52 (2013) 9805−9807.

[149] E. J. O'Neal, C. H. Lee, J. Brathwaite, K. F. Jensen, ACS Catalysis 5 (2015) 2615−2622.

[150] D. Geier, P. Schmitz, J. Walkowiak, W. Leitner, G. Francio, ACS Catalysis 8 (2018) 3297−3303.

[151] T. Touge, M. Kuwana, K. Komatsuki, S. Tanaka, K. Matsumu, N. Sayo, Y. Kashibuchi, T. Saito, Org. Process Res. Dev. 23 (2019) 23 452−461.